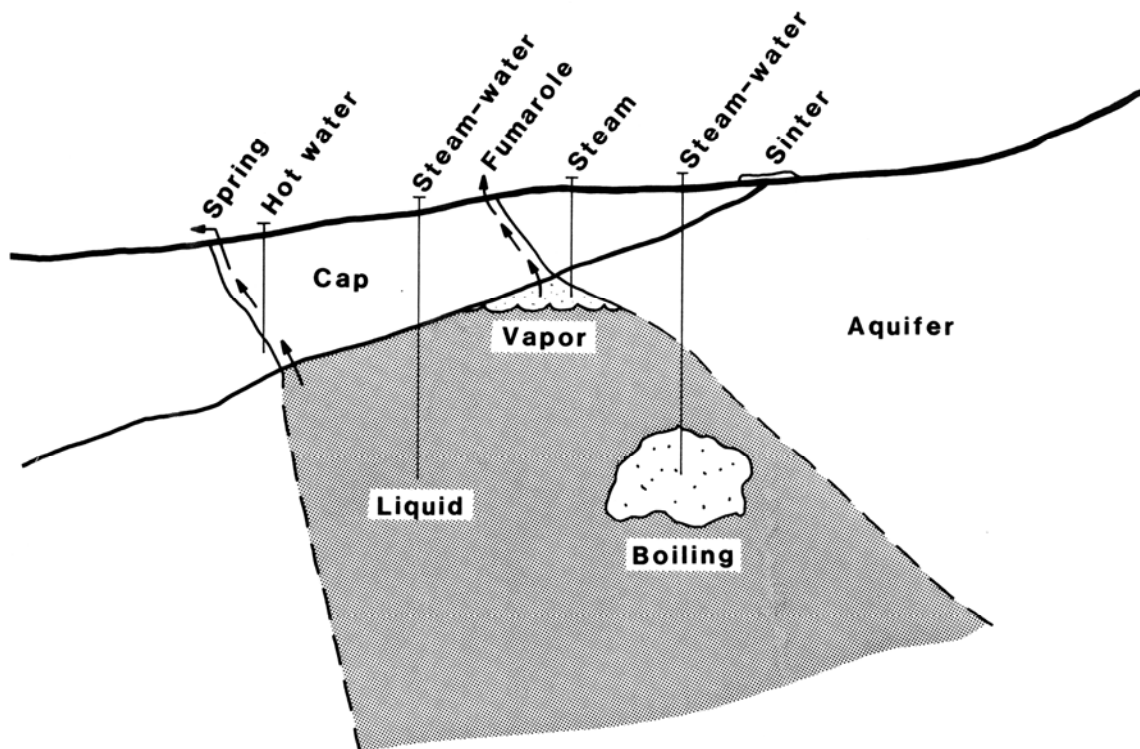


Lecture Notes

GEOHERMAL DELIVERABILITY

Jón Steinar Guðmundsson



Trondheim
July 2009

© Jón Steinar Guðmundsson 2009
Department of Petroleum Engineering and Applied Geophysics
Norwegian University of Science and Technology
7491 Trondheim, Norway

E-post: [jsg\(a\)ipt.ntnu.no](mailto:jsg@ipt.ntnu.no)
Tel: +47 73594952
Fax: +47 73944472

Preface 2009

The present lecture notes have been up-dated and extended from the draft compendium material used last year. The actual lectures last year included material both from the draft compendium and own hand-written notes, as well as additional material in response to the classroom dialogue. Some of the hand-written notes have now been included in the present lecture notes. The 2009 course (GEO604) consist now of three separate courses from 2008. The main new text in the present lecture notes are materials on pressure transient testing (hand-written notes last year). The lecture notes are not yet complete; hand-written materials will supplement the lectures in 2009. Several derivations of equations included last year (Norwegian text) are not included in the present lecture notes. Some of the derivations will be presented during the 2009 lectures. Eight published paper were enclosed in the draft compendium last year. Only two papers are enclosed in the present 2009 version: one paper on geothermal reservoirs and one paper on geothermal wells. (After giving the 15 lectures in one week, the order of the material in the lecture notes was slightly changed and some new material added. The daily exercises are not included in the lecture notes.)

Preface 2008

This draft compendium was put together before giving lectures to students taking the Geothermal Specialization in the The School for Renewable Energy Science at the University of Akureyri in Iceland, July 7-11, 2008. The main message of the lectures is how the concept of Deliverability can be used to study, plan, build and operate geothermal fields and facilities. The Lecture Plan is put together with this in mind, based on own experience from teaching petroleum production at NTNU in Trondheim for many years, the use of geothermal energy at the UN Geothermal Programme in Reykjavik, and courses on geothermal engineering at the University of Iceland and geothermal reservoir engineering at Stanford University in California. Based on an introductory course for non-petroleum engineers at NTNU, materials on reservoir and well topics were included in this compendium. Derivations of equations from own NTNU course on processing of petroleum are included for the specially interested. Unfortunately, most of these are in Norwegian, but since they are derivations, they should not necessarily be difficult to follow (hopefully, some will be translated into English during the time in Akureyri). Finally, the compendium contains selected papers and texts. These should underline the message inherent in the concept of Deliverability.

List of contents

Concept of deliverability	1
Pressure profiles in reservoirs	1
Pressure states in reservoirs	2
Darcy's law	3
Skin factor	4
Superposition	5
Well testing	6
Dimensionless numbers	6
Liquid reservoir performance	7
Liquid inflow performance	8
Step rate testing of wells	9
Skin and deliverability	11
Density of steam, standard conditions and z-factor	11
Steam inflow performance	12
Steam reservoir performance	13
Reservoir temperature	14
Temperature in pipes and wells	15
Pressure profiles in flowing wells	16
Outflow performance	17
Static pressure in wells	17
Pressure drop in pipes and wells	17
Two-phase wells and pipelines	19
Pumps and pumping	19
Artificial lift	23
Pressure transient analysis	24
Two-phase flow variables	30
Two-phase homogeneous flow	32
Slip ratio equation	34
Conversion factors	36
Paper: Composite model of geothermal reservoirs	
Paper: Two-phase wells	

Concept of deliverability

- Analyze individual performances and then synthesize to get deliverability
- Methodology to estimate capacity of wells and field to deliver fluids
- Rate, q , and pressure, p , main parameters
- Reservoir performance, reservoir pressure against cumulative production
- Inflow performance, down hole pressure against flow rate
- Outflow performance, tubing performance, down hole pressure at fixed wellhead pressure (several curves for different wellhead pressures)

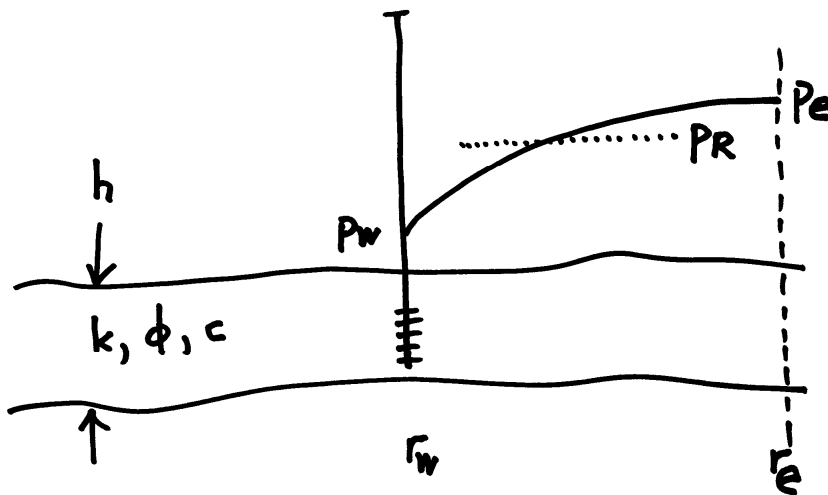
Deliverability and Performances

Pressure Profile from Reservoir to Wellhead

- Reservoir performance gives reservoir pressure against cumulative production (or average reservoir pressure with time). For example, p/z method for simple gas reservoirs.
- Inflow performance gives downhole flowing pressure against well production rate. Practically equal to reservoir pressure when no production (well shut-in).
- Tubing performance gives the pressure drop from downhole to wellhead. Assuming a wellhead pressure, the downhole pressure can be calculated (compressible flow in pipes) for different well production rates. One curve for each wellhead pressure.
- Deliverability is the overall effect of the reservoir, inflow and tubing performances.

Pressure profile in reservoir

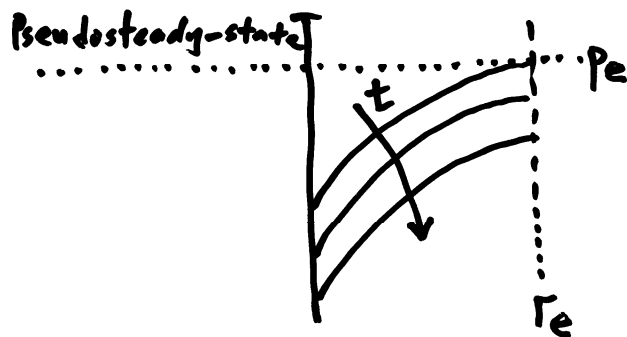
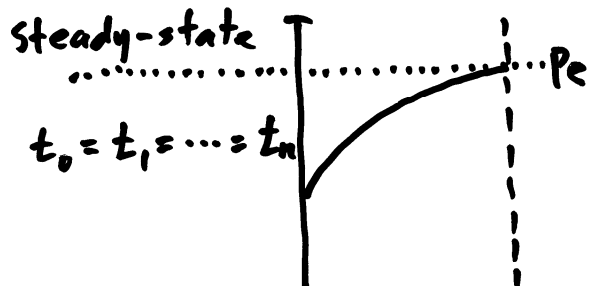
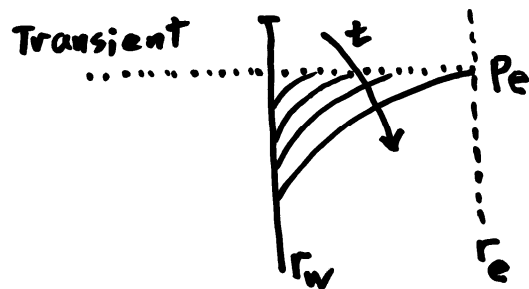
Pressure profile from r_w til r_e , from well radius to outer boundary. Drainage area (and drainage volume) extends from well to outer boundary.



k = permeability [m^2]
 ϕ = porosity [-]
 c = compressibility [Pa^{-1}]
 h = reservoir thickness [m]
 r_w = well radius [m]
 r_e = reservoir radius (radial system, e = exterior) [m]
 $p_w = p_{wf}$ well pressure (wf = well flowing) [Pa]
 p_e = pressure at outer boundary (exterior) [Pa]
 p_R = reservoir pressure [Pa]

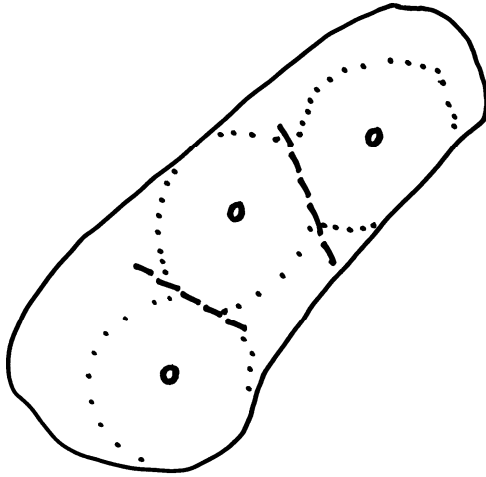
Pressure states in reservoirs

- Transient state (TS)
- Steady-state (SS)
- Pseudosteady-state (PSS)



PSS occurs when pressure profiles meet (at the drainage boundary). It is the most common state in production of fluids from subsurface reservoirs. TS occurs when wells are started-up or shut-down. The TS is used to test the flow properties of wells, both the flow capacity and storage capacity of the formation.

Figure below shows areal view of a reservoir with three production wells, illustrating the drainage area and drainage boundary.



Darcy's law

Assuming steady-state flow through porous media, the flowrate (expressed as fluid velocity) is proportional to permeability and pressure gradient. And, the more viscous the fluid, the lower the flowrate.

$$u = -\frac{k}{\mu} \frac{dp}{dr}$$

u = Darcy velocity = filtration velocity (based on the whole area; that is, not only the pore spaces). An analogy to superficial velocity in two-phase flow in pipes.

$$q = uA$$

$$A = 2\pi rh$$

Integrates from r and p to r_w and p_{wf} , thus minus cancelled out.

$$p = p_{wf} + \frac{\mu q B}{2\pi k h} \ln\left(\frac{r}{r_w}\right)$$

$$q = q_{s.c.} B$$

$$B = \frac{V}{V_{s.c.}}$$

- Reservoirs have properties k, ϕ, h, c
- Wells have property s
- Well testing gives kh (permeability thickness), the flow capacity
- Well testing gives ϕch (porosity-compressibility thickness), the storage capacity

Volumetric flow q stands for rate at local conditions (*in situ*). Volumetric flow $q_{s.c.}$ stands for rate at standard conditions. In the U.S. these are 1 atmospheric pressure and 60 F, while in Norway these are 1 atmospheric pressure and 15 C.

The factor B is the formation volume factor. It expresses how the volume of fluid changes from reservoir to surface separator. It is quite important in oil production because it takes into account the volume reduction of oil as dissolved gas evolves. In the low-temperature geothermal case, the change in liquid water volume from reservoir to surface is quite small. In the liquid-dominated high-temperature geothermal case, the steam fraction changes from reservoir to surface; calculated from Steam Tables. In the vapour-dominated high-temperature geothermal case, the steam volume changes from reservoir to surface, similar to natural gas production.

The concept of relative permeability is not covered in the present lecture notes.

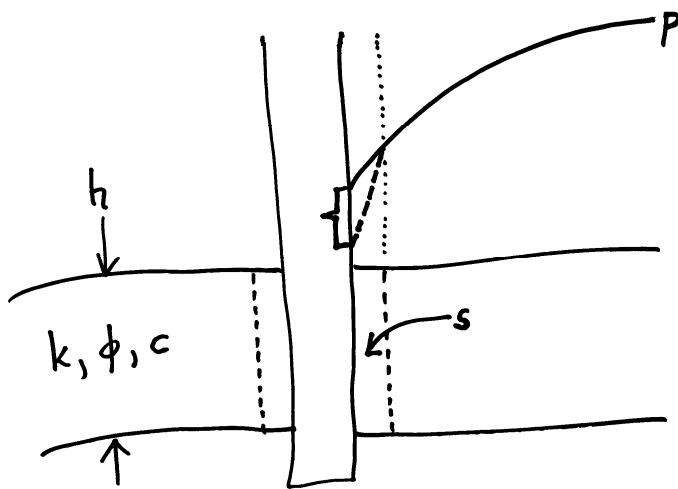
Skin factor

- Increases or decreases the pressure drop near wellbore
- Expresses pressure drop deviating from an ideal well behaviour
- Constant for a particular well
- Damage, near-wellbore, $s > 0$
- Stimulated, near-wellbore, $s < 0$
- Geometric skin, $s > 0$
- Fracture skin, $s < 0$
- Deposits, $s > 0$

The skin factor can arise because of several types of skin (damage, fracture, geometry etc.). In such cases the skin factor is constant. There can also be a rate dependent skin, for example due to high-velocity flow effects. Rate dependent skin is not discussed here.

Constant skin can be expressed in terms of apparent well radius as

$$r_{wa} = r_w e^{-s}$$



Superposition

- The total pressure drop at any point in a reservoir is the sum of the pressure drops at that point caused by the flow in each of the wells in the reservoir.
- Applies in all pressure states, TS, SS and PSS.
- The diffusivity equation describes the pressure distribution in a reservoir with time and distance. The solution to the diffusivity equation is linear; therefore, the pressure values can be added.
- The principle of superposition can also be used to take into account the presence of faults, by using image wells.

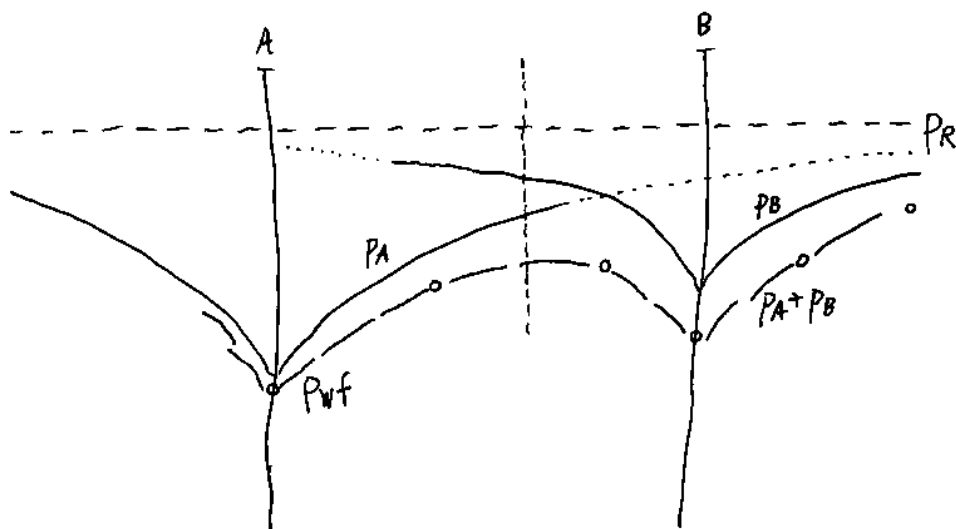


Figure – Pressure profiles for well A and well B alone (individually) are shown as p_A and p_B . In superposition the individual drawdowns are added, here shown as $p_A + p_B$. The drainage boundary between the wells is shown as vertical line.

Well testing

- Pressure transient analysis, constant q , variable p
- Decline curve analysis, constant p , variable q
- Step rate testing, p and q at different near-steady values

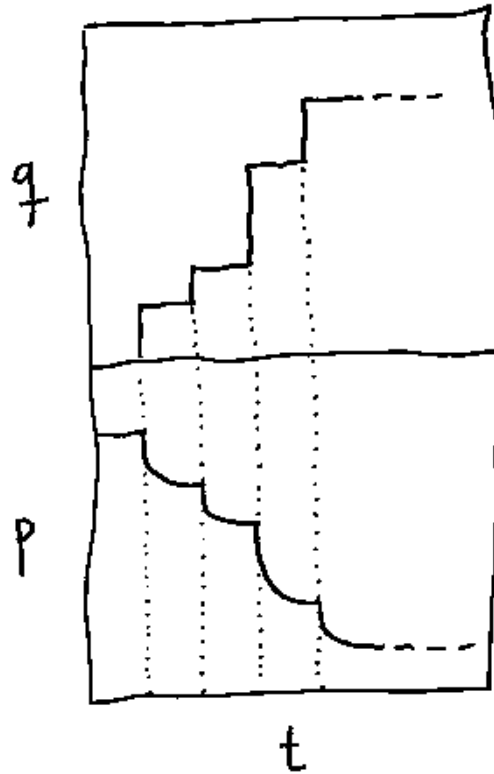


Figure – Step rate testing, each interval step change run long enough for stable q and p .

Dimensionless numbers

$$p_D = \frac{2\pi kh}{qB\mu} \Delta p$$

$$t_D = \frac{kt}{\phi\mu c_i r_w^2} = \frac{kh}{\phi c_i h} \frac{t}{\mu r_w^2}$$

$$r_D = \frac{r}{r_w}$$

Liquid reservoir performance

- Pressure with time (cumulative production)
- Usual state PSS (when no injection)
- p_R decreases with time, or with N_p , cumulative production
- p_i is initial reservoir pressure (at some reference depth)

$$N_p B = V c_t (p_i - p_R)$$

V is the fluid filled pore volume and c_t the total (formation and fluid) compressibility.

$$c_t = c_f + S_w c_w$$

In low-temperature reservoirs, the pore volume is filled with water such that $S_w=1$.

$$p_R = p_i - \frac{qB}{A\phi c_t h} t$$

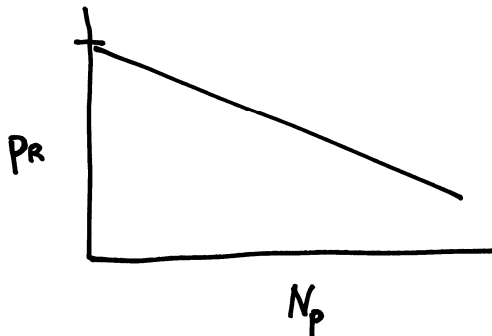
Isothermal compressibility of fluid is defined by

$$c = \frac{-1}{V} \left(\frac{dV}{dp} \right)_T$$

In oil reservoirs, the total compressibility $c_t = S_o c_o + c_f$ where S stands for saturation and f for formation. If oil and gas and water are produced together, the total compressibility is given by the relationship

$$c_t = c_f + S_o c_o + S_g c_g + S_w c_w$$

In the geothermal case, the appropriate compressibility values need to be used. In steam-dominated reservoirs, there is adsorbed liquid water on the formation rock, making the steam content larger than simple pore volume.



Reservoir pressure decreases with increased liquid production. The recoverable liquid is less than the liquid originally in place. Water influx makes reservoir pressure decrease less rapidly.

It is less helpful to plot p_R with time because the fluid withdrawal rate most likely varies with time, e.g. from winter to summer. On a p_R with time t plot, therefore, the line will not be as straight as on a p_R with cumulative production plot.

Above the fluid is produced due to expansion from reservoir pressure to wellbore pressure (confined reservoir volume). Geothermal reservoirs are characterised by extensive (vertical) fracturing such that there are fluid openings between the reservoir and the surface. The reservoir can therefore be considered as an open tank where the fluid level decreases as fluids are removed. In such as case fluids are not produced due to expansion; that is, the porosity-compressibility-thickness product (storativity) does not determine the slope of the reservoir pressure against cumulative production plot. In open (unconfined) reservoirs the storativity is given by the porosity-divided-by-(density×gravity constant). Unconfined reservoir models are not included in the present lecture notes.

Liquid inflow performance

- PSS rate equation

$$q = \frac{2\pi kh(p_R - p_{wf})}{\mu B \left[\ln\left(\frac{r_e}{r_w}\right) - 3/4 + s \right]}$$

- Productivity index

$$q = PI(p_R - p_{wf})$$

$$PI = \frac{2\pi kh}{\mu B \left[\ln\left(\frac{r_e}{r_w}\right) - 3/4 + s \right]}$$

- PSS pressure equation

$$p_{wf} = p_R - \frac{\mu q B}{2\pi kh} \left[\ln\left(\frac{r_e}{r_w}\right) - 3/4 + s \right]$$

Reservoir pressure p_R above and elsewhere is the volume average reservoir pressure given by

$$P_R = \frac{\int_{r_w}^{r_e} p dV}{\int_{r_w}^{r_e} dV}$$

The constant $3/4$ arises when the volume average pressure is used in PSS. In SS the constant is $1/2$.

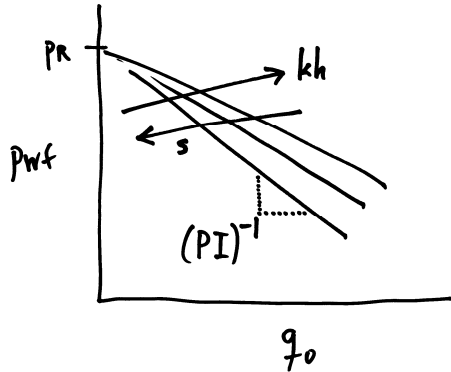


Figure – Increasing kh increases flowrate, increasing s decreases flowrate. Gradient is equal to $(-1/PI)$.

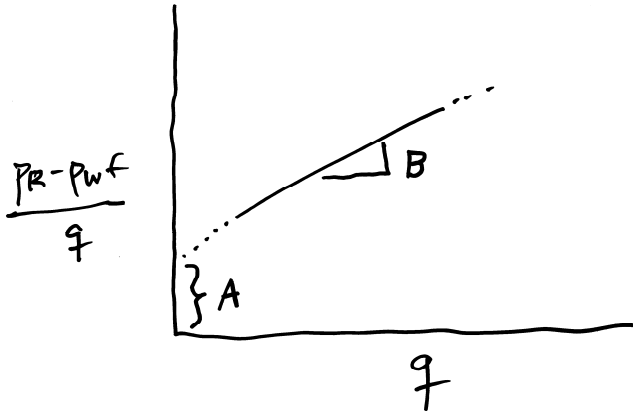
Step rate testing of wells

Liquid systems:

$$p_R - p_{wf} = Aq + Bq^2$$

The first part on the RHS, Aq , expresses the pressure drop due to Darcy flow. The second part on the RHS, Bq^2 , expresses the pressure drop to high-velocity flow. Dividing by q gives

$$\frac{p_R - p_{wf}}{q} = A + Bq$$



Steam systems (and low-pressure natural gas):

$$\frac{p_R^2 - p_{wf}^2}{q} = A + Bq$$

The backpressure equation

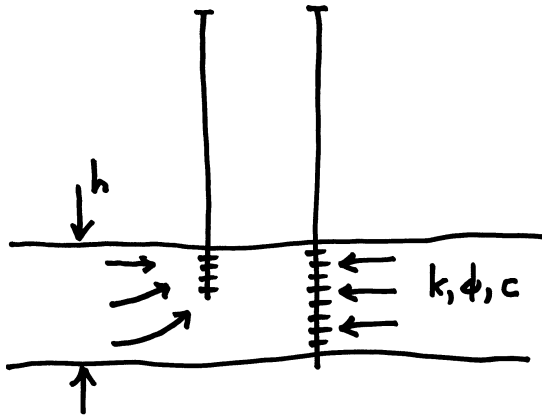
$$q = C(p_R^2 - p_{wf}^2)^n$$

can also be used, especially for steam wells. C and n are the backpressure coefficient and exponent, respectively. The value n usually in the range 0.5 to 0.7.

Skin and deliverability

- Reservoir performance
- Inflow performance
- Outflow performance

Imagine two nearby wells in a heterogeneous reservoir. One of the wells is fully penetrating while the other well is partially penetrating. The production tubing in the wells are identical. Therefore, the reservoir performance and the outflow performance of the two wells are the same, but the inflow performances are different; this due to geometric skin.



Density of steam, standard conditions and z-factor

Real gas law

$$pV = znRT$$

Gas density

$$\frac{n}{V} (\text{mol} / \text{m}^3) = \frac{p}{zRT}$$

$$\rho (\text{kg} / \text{m}^3) = \frac{pM}{zRT}$$

$$M (\text{kg} / \text{kmol})$$

Standard conditions (s.c.)

$$n = n_{s.c.}$$

$$\frac{pV}{zRT} = \frac{p_{s.c.}V_{s.c.}}{z_{s.c.}RT_{s.c.}}$$

$$z_{s.c.} = 1$$

$$V = V_{s.c.} \left(\frac{p_{s.c.}}{p} \right) \left(\frac{T}{T_{s.c.}} \right) z$$

$$q = q_{s.c.} \left(\frac{p_{s.c.}}{p} \right) \left(\frac{T}{T_{s.c.}} \right) z$$

$$B_g (=FVF \text{ gas}) = \frac{V}{V_{s.c.}} = \left(\frac{T}{T_{s.c.}} \right) \left(\frac{p_{s.c.}}{p} \right) z$$

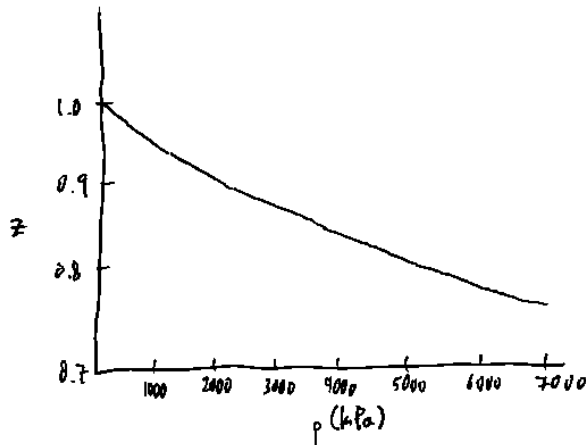


Figure – Compressibility factor (z-factor) for saturated steam (illustration, not accurate).

Steam inflow performance

Rate equation from Darcy's Law

$$q = \frac{2\pi kh}{\ln\left(\frac{r_e}{r_w}\right)} \left(\frac{T_{s.c.}}{T} \right) \left(\frac{1}{p_{s.c.}} \right) \int_{p_{wf}}^{p_e} \left(\frac{p}{\mu_g z} \right) dp$$

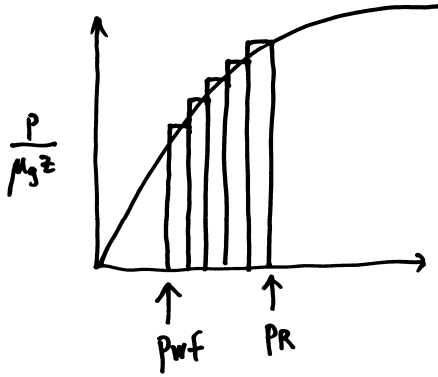
Rate equation from Darcy's Law for PSS and skin. Note that the integration is from p_{wf} (well flowing pressure) as above but now to p_R (volume average reservoir pressure)

$$q = \frac{2\pi kh}{\left[\ln\left(\frac{r_e}{r_w}\right) - 3/4 + s \right]} \left(\frac{T_{s.c.}}{T} \right) \left(\frac{1}{p_{s.c.}} \right) \int_{p_{wf}}^{p_R} \left(\frac{p}{\mu_g z} \right) dp$$

- Solution method, the pressure function (also called property function), because steam (gas) viscosity and z-factor change with pressure

$$F(p) = \left(\frac{p}{\mu z} \right)$$

Integration numerically between p_R and p_{wf}



- Specific/limiting solutions

Low pressure, pressure function increases linearly with pressure such that (as in the back-pressure equation). The case for geothermal steam.

$$" \Delta p " = p_R^2 - p_{wf}^2$$

High pressure, pressure function constant (same expression as for oil and water)

$$" \Delta p " = p_R - p_{wf}$$

The pressure function (property function) at low pressure, as in vapour dominated steam reservoirs, is linear with pressure. Therefore

$$\int_{p_{wf}}^{p_R} \left(\frac{p}{\mu z} \right) dp = \left(\frac{1}{\mu z} \right) \int_{p_{wf}}^{p_R} p dp = \left(\frac{1}{\mu z} \right) \frac{1}{2} (p_R^2 - p_{wf}^2)$$

Note that the factor 2 cancels out when this expression is used in the rate equation for steam wells.

Steam reservoir performance

Vapour dominated reservoir

$$pV = zmRT$$

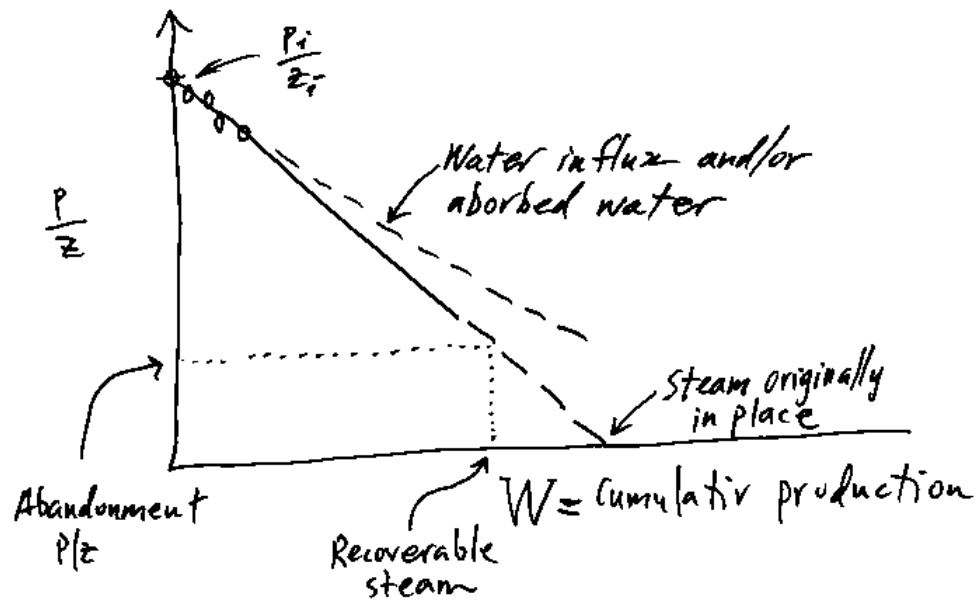
$$n = \frac{W}{M}$$

where W is mass of steam. Assume reservoir V constant and reservoir T constant

$$pV = z \frac{W}{M} RT$$

$$\frac{p}{z} \propto W$$

$$\frac{p}{z} = \frac{p_i}{z_i} \left(\frac{W_i - W}{W_i} \right)$$



Figur – p/z method for vapour dominated steam reservoirs.

Reservoir temperature

- Temperature with depth
- Figure immediately below shows conduction only (no convection)
- Fourier's Law

$$q = -kA \frac{dT}{dx}$$

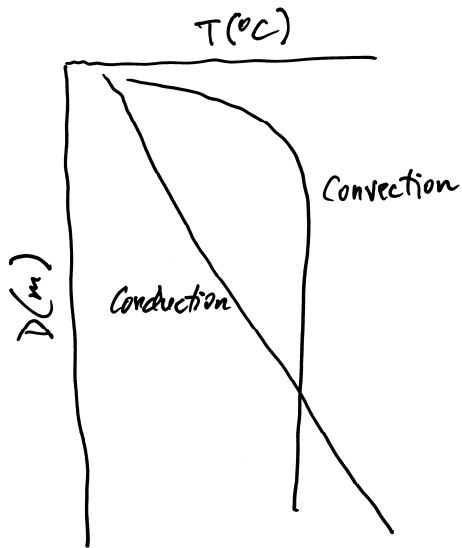
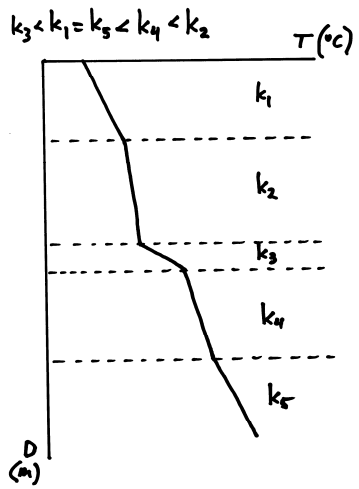
q = heat flow [W = J/s]

A = area [m²]

k = thermal conductivity [W/m.K]

T = temperature [K]

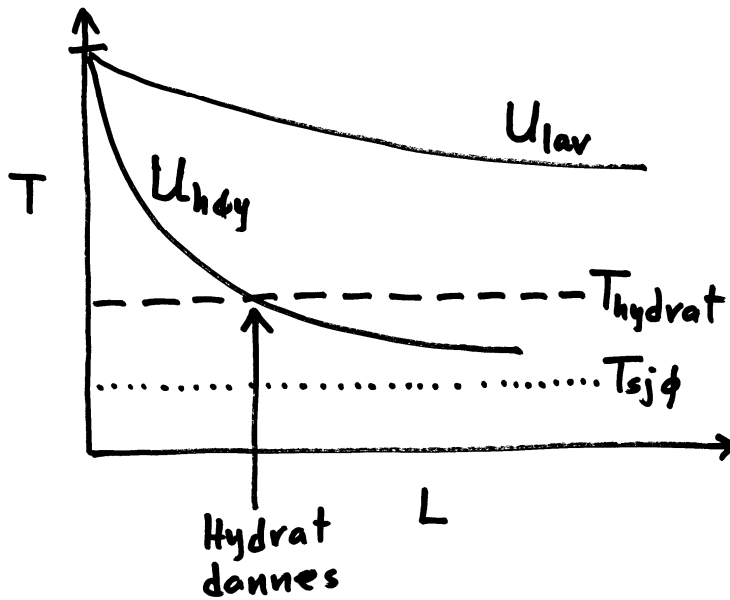
x = distance [m]



Temperature in pipes and wells

- Inlet T_1 , outlet T_2 , environment (air, soil, water) T

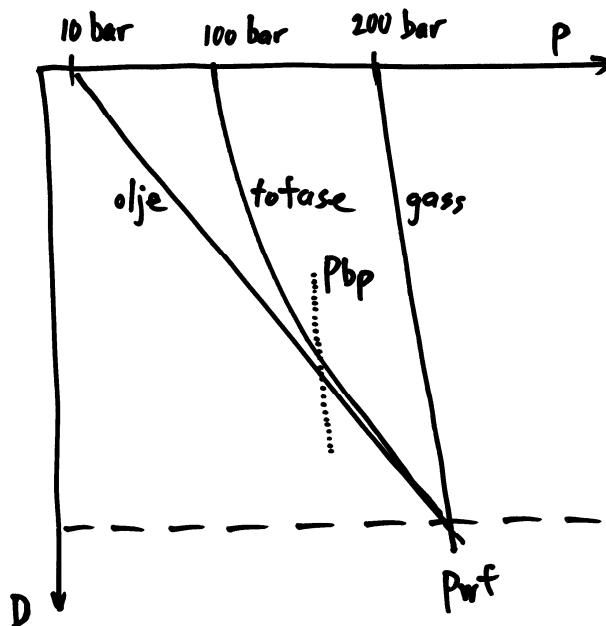
$$T_2 = T + (T_1 - T) \exp\left[\frac{-U\pi d}{mC_p} L\right]$$



- Insulated pipelines, $1 < U < 2$ (W/m^2K)
- Non-insulated pipelines, $15 < U < 25$ (W/m^2K)

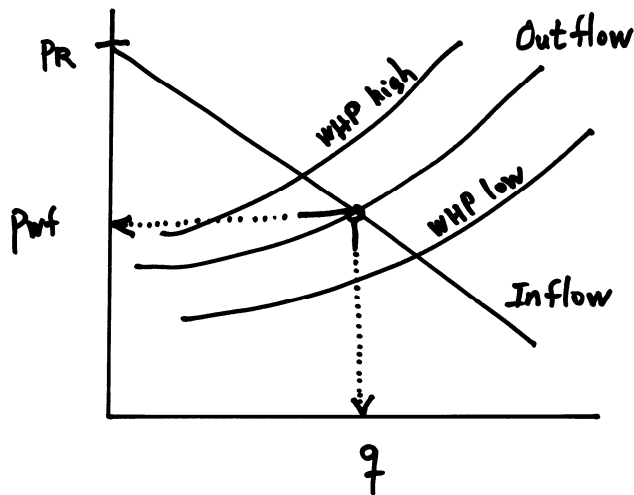
Pressure profiles in flowing wells

- Liquid only (oil or water)
- Vapour only (gas or steam)
- Two-phase well with boiling point in wellbore (oil well with bubble point in production tubing)



Outflow Performance

- Outflow performance, also called vertical lift performance
- Pressure drop measured/calculated from wellhead to bottomhole (from p_{th} = tubing head pressure to p_{wf})
- Analytical equations and/or wellbore flow packages can be used for calculations
- Each curve for each wellhead pressure (and, one production tubing design)
- Production rate given by point where inflow and outflow curves meet.



Static pressure in wells

- Liquid only

$$p = \rho g L$$

- Vapour only (use average values of z and T , from wellhead to bottomhole)

$$p = p_o \exp\left[\frac{gM}{zRT} L\right]$$

To solve, assume average z and average T , then iterate.

Pressure drop in pipes and wells

- Total pressure drop, friction + hydrostatic (gravity) + acceleration
-
- $\Delta p = \Delta p_f + \Delta p_g + \Delta p_a$
- Pressure drop due to acceleration

$$\Delta p_a = \rho u \Delta u$$

- Hydrostatic pressure drop

$$\Delta p_g = \rho g \Delta h$$

where Δh is the height difference between outlet and inlet; that is, not thickness of reservoir.

- Darcy-Weisbach equation for liquids (incompressible fluid), wall friction

$$\Delta p_f = \frac{f}{2} \frac{L}{d} \rho u^2$$

- Compressible fluids, wall friction

-

$$\frac{dA^2 M}{f m^2 z RT} (p_2^2 - p_1^2) - \frac{d}{f} \ln \left(\frac{p_2^2}{p_1^2} \right) + L = 0$$

For typical pipelines, the logarithmic part can be ignored.

- Friction factor

Smooth pipes, Blasius' equation when $Re < 10^5$.

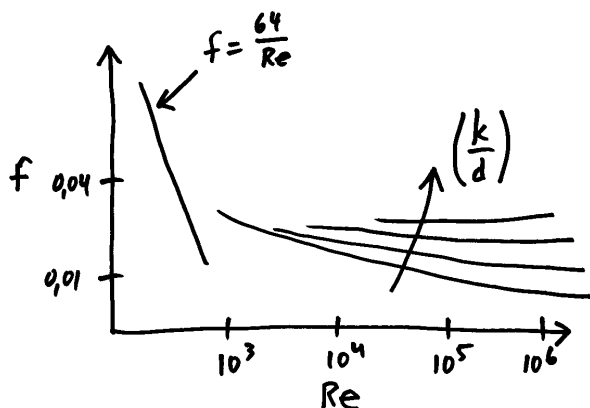
$$f = \frac{0,316}{Re^{0,25}}$$

$$Re = \frac{\rho u d}{\mu}$$

Rough pipes, Haaland's equation, for general use.

$$\frac{1}{\sqrt{f}} = -\frac{1,8}{n} \log \left[\left(\frac{6,9}{Re} \right)^n + \left(\frac{k}{3,75d} \right)^{1,11n} \right]$$

$n = 1$ for liquids, $n = 3$ for gas and steam



Material	Average Absolut Roughness (inch)	Average Absolut Roughness (μm)
Internally plastic coated pipeline	0.200×10^{-3}	5.1
Honed bare carbon steel	0.492×10^{-3}	12.5
Electropolished bare 13Cr	1.18×10^{-3}	30.0
Cement lining	1.30×10^{-3}	33.0
Bare carbon steel	1.38×10^{-3}	35.1
Fiberglass lining	1.50×10^{-3}	38.1
Bare 13Cr	2.10×10^{-3}	53.3

Two-phase wells and pipelines

This material was not covered. However, basic equations for two-phase flow are given at the back of this text.

Pumps and pumping

Types of pumps

- Volumetric (piston pump)
- Dynamic (centrifugal pump)
 - Rate depends on diameter
 - Pressure depends on number of stages (wheels)

Pressure and head are used

$$p = \rho gh$$

$$h = \frac{p}{\rho g}$$

Ideal pump power (unit W)

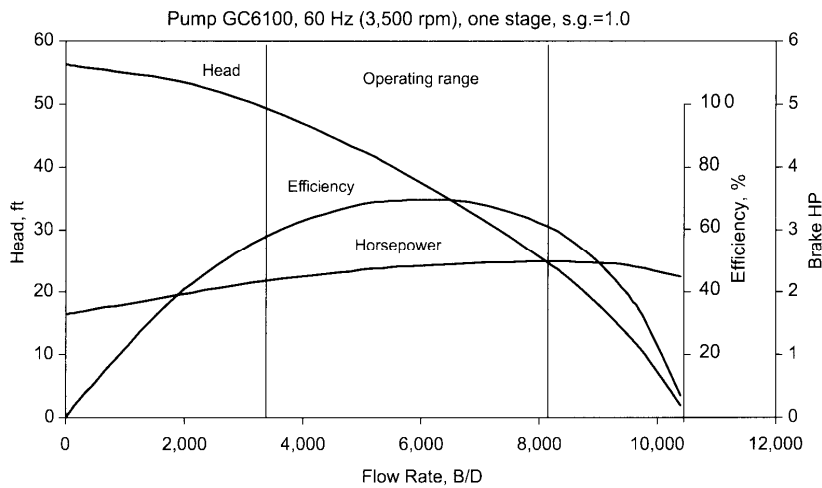
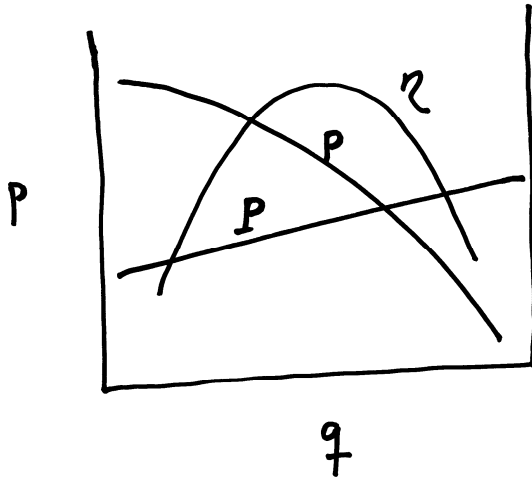
$$P = q\Delta p$$

Real pump power

$$P = q\Delta p \frac{1}{\eta}$$

where η is efficiency, typically 0.8 at design conditions.

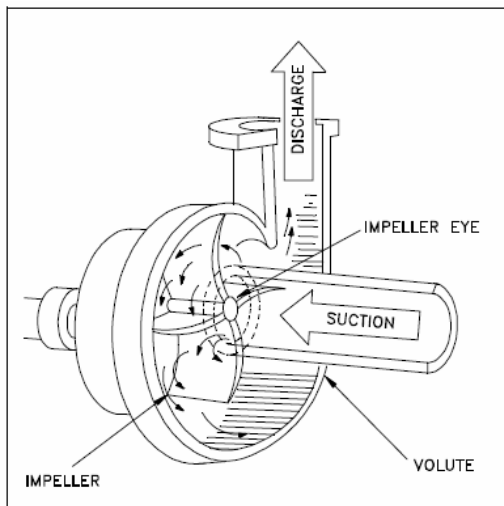
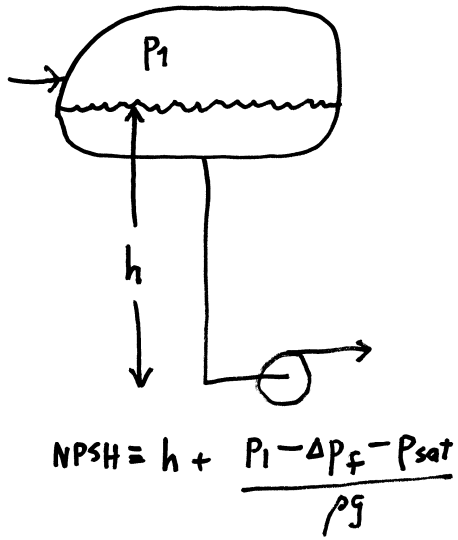
Characteristic curve (centrifugal pump)



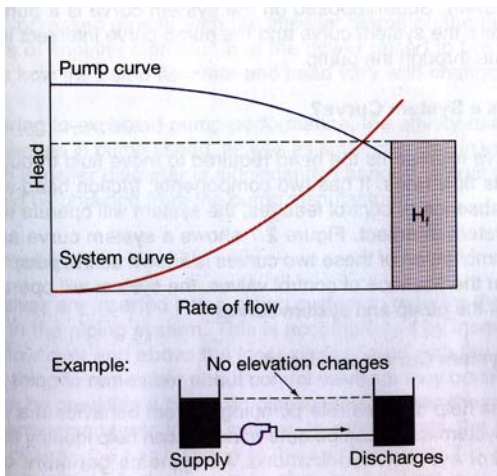
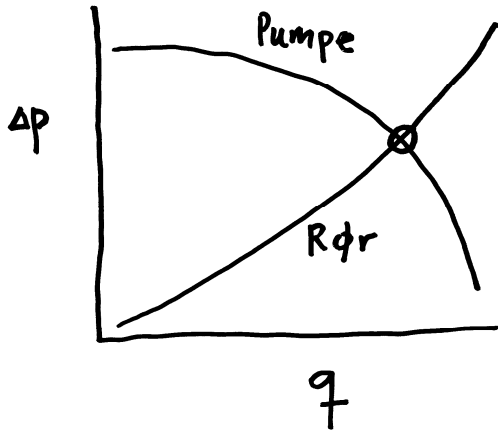
Curves from manufacturer (Pessoa & Rado, SPE Production & Facilities, February 2003)

Cavitation and suction head

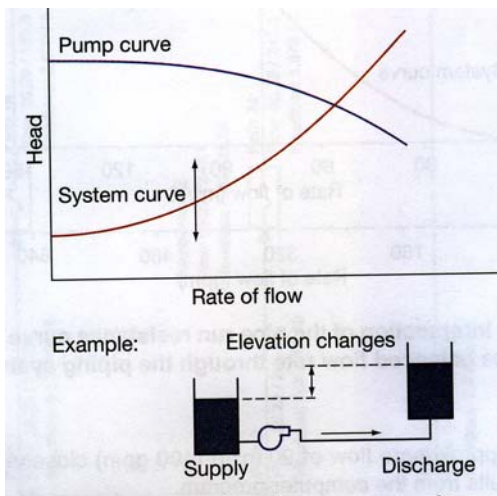
- All pumps must have high enough inlet pressure, otherwise the fluid will start to boil
- Cavitation, bubbles created and collapse
- Head to a pump is height minus friction (from open tank)
- NPSH = Net Positive Suction Head, specified by manufacturer
- When p_1 is equal to p_s (saturation pressure) a special case
- Heat of vaporisation of water is higher than for hydrocarbons



Centrifugal pump (DoE 1993).



System curve resulting from only friction (Hydraulic Institute 2008).

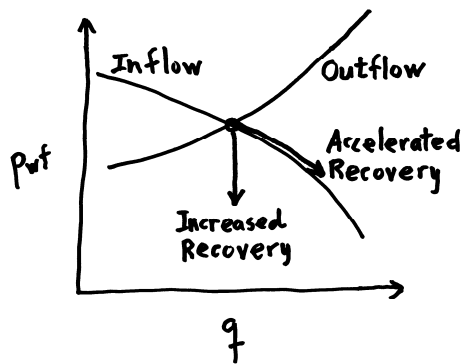
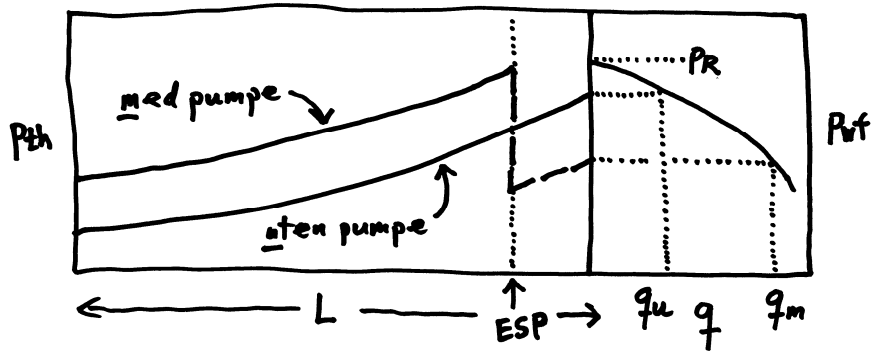


Effect of elevation changes on system curve (Hydraulic Institute 2008).

Artificial lift

With and without ESP (electrical submersible pump)

- Vertical pressure profile, p_t (pressure in tubing)
- Wellhead pressure, p_{th} (= WHP)
-



Downhole pumps can increase the flow rate and Accelerate Recovery and/or Increase Recovery.

Pressure transient analysis

The transient state of a well can last for less than an hour to more than several days. During this time the well pressure and flow rate change with time. How the pressure and flow rate change with time depends on the nature of the well-reservoir system. If the flow rate is kept constant during the transient state, pressure transient analysis can be performed, also call well test analysis. If the well pressure is kept constant during the transient state, decline curve analysis can be performed. In real testing situations it is difficult to keep the flow rate or well pressure constant. In modern well test analysis the principle of superposition and appropriate computer programme are used to compensate for variations with time in well pressure and flow rate. To illustrate the use of pressure and/or flow rate transients it is convenient to assume one of these parameters as constant. In the following, the flow rate is assumed constant.

The transient state can be used to extract information about a well-reservoir system, including:

- Permeability-thickness kh in drainage volume of well
- Porosity-thickness-product ϕch or storativity of drainage volume
- Condition of well represented by skin factor s (whether well is damaged or stimulated)
- Average reservoir pressure p_R within the drainage volume, at the time of testing
- Reservoir geometry, faults, fractures, gas-liquid interfaces.

Pressure transient analysis as presented here is that used by petroleum engineers in the oil and gas industry. Pressure transients are also used in the groundwater hydrology industry. While the theoretical basis is the same in both industries, the terminology is not identical. Both terminologies are used in the geothermal industry. In the petroleum industry Darcy's Law is commonly written

$$u = \frac{-k}{\mu} \frac{dp}{dr}$$

while in groundwater hydrology it is commonly written

$$u = -K \frac{dh}{dr}$$

because the concept of head, h , is used. The symbol K stands for permeability and is related to intrinsic permeability by

$$k = K \frac{\mu}{\rho g}$$

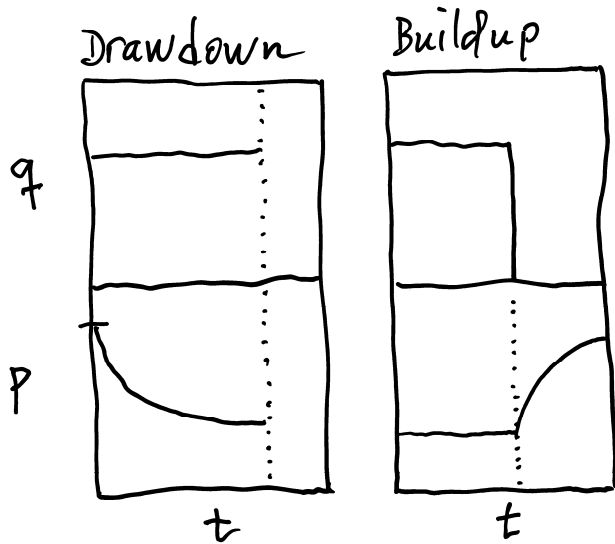
In the present text the intrinsic permeability k (m^2) will be used and called, just, permeability. This permeability is sometimes called hydraulic conductivity. The permeability K (m^2/s) in groundwater hydrology is used in the definition of transmissivity $T = Kh$.

Several types of tests are used in pressure transient analysis. Single well tests include:

- Drawdown test, production well
- Buildup test, production well
- Injectivity test, injection well
- Falloff test, injection well

Multiple well tests include:

- Interference test, active well
- Interference test, observation well



The above figure shows a drawdown test where the flow rate is kept constant and the well pressure decreases with time. The figure shows also a buildup test where the well has been on-stream long enough for the well pressure to stabilize. The well pressure increases when the well is shut-in (closed). Both drawdown and buildup transients can be used to determine the properties of well-reservoir systems.

The partial differential equation that describes the propagation of a pressure wave with time in a reservoir formation subject to fluid production (or injection) is the simplified diffusivity equation

$$\frac{\partial^2 p}{\partial r^2} + \frac{1}{r} \frac{\partial p}{\partial r} = \frac{\phi \mu c_i}{k} \frac{\partial p}{\partial t}$$

It is one-dimensional because it includes only radial distance. Pressure changes are assumed small and Darcy's Law applies. The system is slightly compressible and the fluid viscosity is constant. The reservoir engineering parameters on the right-hand side are called hydraulic diffusivity

$$\eta = \frac{k}{\phi \mu c_i}$$

The diffusivity equation is used to describe all kinds of diffusivity processes. The solution of the diffusivity equation involves what is called the exponential integral, E, and can be written as follows

$$p(r,t) - p_i = \frac{-q\mu}{4\pi kh} E\left(\frac{\phi\mu c_i r^2}{4kt}\right)$$

Reservoir pressure at any distance r and at any time t, p(r,t), depends on the flow rate, formation properties, fluid properties and the solution of E. An exact and complete solution of E is not available so approximate solutions are used, appropriate for different time spans. The following solution can be used in pressure transient testing

$$E(x) \cong -\ln(x) - \gamma$$

where γ is Eulers constant 0.5772 (the limiting difference between the harmonic series and the natural logarithm). The E solution is appropriate for $x < 0.01$ representing large values of time or small distances, such as a wellbore.

$$p - p_i = \frac{-q\mu}{4\pi kh} \left[\ln(t) + \ln\left(\frac{4k}{\phi\mu c_i r^2}\right) - \gamma \right]$$

The groups k/μ , kh/μ and ϕch are in petroleum engineering called mobility, mobility thickness and storativity, respectively.

Using logarithm to base 10 the equation can be written as

$$p - p_i = -m \left[\log t + \log\left(\frac{4k}{\phi\mu c_i r^2}\right) - 0.2507 \right]$$

where

$$m = \frac{2.303q\mu}{4\pi kh}$$

If the pressure difference $p-p_i$ is plotted against $\log(t)$ the slope of the line will be m (determined from plot). Assuming the flow rate q is constant, the mobility thickness can be determined from

$$\frac{kh}{\mu} = \frac{2.303q}{4\pi m}$$

At some time t, the solution of the pressure transient equation can be written

$$\frac{p - p_i}{m} = -\log \left[\left(\frac{4kh}{\mu} \right) \left(\frac{1}{\phi ch} \right) \left(\frac{t}{r^2} \right) \right] + 0.2507$$

It follows that the storativity can be determined from

$$\phi c h = 2.25 \left(\frac{kh}{\mu} \right) \left(\frac{t}{r^2} \right) 10^{\left(\frac{p-p_i}{m} \right)}$$

The above solution of the diffusivity equation has different names in different fields of study. In petroleum engineering it is called line-source solution. In groundwater hydrology it is called Theis solution. In other fields of study the solution is sometimes called Kelvin's point source.

The above equations are presented using SI units. Oil field units are commonly used in the oil and gas industries, such that the constants have different values. Other units can also be used in groundwater hydrology.

In the above equations the radius r is usually the well radius where the pressure is measured. In interference testing, where the pressure is measured at some distance (distance between active well and observation well) the radius value used is the same distance. The compressibility above is the total compressibility c_t . The volumetric flow rate q is the local flow rate (down hole). If flow rate at standard conditions is used, as common, the formation volume factor needs to be applied.

The diffusivity equation is a linear partial differential equation, which means that the pressure values (effects) are additive. Therefore, the principle of superposition can be used. For a well that has produced for time t and then shut-in for time Δt . For time $t+\Delta t$ the exponential integral solution can be written

$$p(r, t) - p_i = \frac{-q\mu}{4\pi kh} E\left(\frac{\phi\mu c_t r^2}{4kt}\right) - \frac{-q\mu}{4\pi kh} E\left(\frac{\phi\mu c_t r^2}{4k\Delta t}\right)$$

Following the same derivation as above gives the result

$$p - p_i = \frac{2.303q\mu}{4\pi kh} \log\left(\frac{t + \Delta t}{\Delta t}\right)$$

A plot of pressure against the logarithm of the time ratio is called a Horner-plot. When extended/extrapolated to 1, the initial reservoir pressure (average reservoir pressure) can be estimated. Symbol p^* is commonly used for this extrapolated pressure.

The line-source solution can be written using dimensionless numbers, resulting in

$$p_D = \frac{1}{2} [\ln t_D + 0.80907]$$

The dimensionless equation is used in type-curve matching. It can also be used to illustrate how the skin factor, s , can be included. The skin factor is constant and is dimensionless such that

$$p_D = \frac{1}{2} [\ln t_D + 0.80907] + s$$

Another way to express the effect of skin is to write the resulting additional pressure drop as

$$\Delta p_s = \frac{q\mu}{2\pi kh} s$$

Because skin represent additional pressure drop it can be added to the line-source solution equation

$$p - p_i = -\frac{2.303q\mu}{4\pi kh} \left[\log t + \log \left(\frac{4k}{\phi\mu cr^2} \right) - 0.2507 + 0.8686s \right]$$

In principle, any point on a semilog (log-linear) line can be used to determine skin factor s . It is customary in the petroleum industry to calculate when the logarithm of 1 is zero. Using SI unit, the above equation can be solved for the skin value, s , using all other measured values at 1 second. But at 1 second the well has not reached the time span where the line-source solution applies. The line-source solution results in a straight line on a semilog plot (linear pressure against logarithm of time). Therefore, the straight line must be extrapolated to 1 second. Rearranging the above equation to calculate skin gives

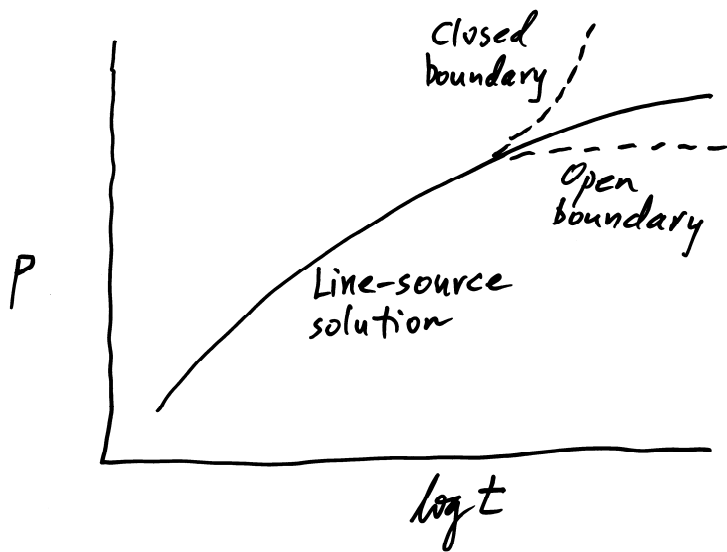
$$s = 1.151 \left[\frac{p_i - p_{1\text{sec}}}{m} - \log \left(\frac{4k}{\phi\mu cr^2} \right) + 0.2507 \right]$$

When using oil field units, the unit of time is hour, which may result in more realistic values of the measured parameters.

$$s = 1.151 \left[\frac{p_i - p_{1\text{hr}}}{m} - \log \left(\frac{k}{\phi\mu cr^2} \right) + 3.2274 \right]$$

Traditional oil field units are the following:

- k = permeability (md)
- h = thickness (feet)
- p_i = initial reservoir pressure (psi)
- p_{wf} = well flowing pressure (psi)
- q = production rate (STB/d)
- B = formation volume factor (res vol/std vol)
- μ = viscosity (cp)
- t = time (hour)
- ϕ = porosity (pore vol/bulk vol)
- c = compressibility (1/psi)
- r = radius (ft)



The line-source solution is infinite acting. With time the pressure change will reach the outer boundary of a drainage volume. If the outer boundary is open, the pressure will flatten out (not usual). If the outer boundary is closed, the pressure will change more rapidly (usual, for example PSS). Pressure measurements at the start will also include the effect of wellbore fluid, called wellbore storage; it masks the pressure response of the reservoir formation. Wellbore storage is characterized with unit slope on a log-log plot. The slope m must be taken after the wellbore storage effect has disappeared from the data.

Wellbore storage constant C , drainage volume shape factor C_A are not covered in the present lecture notes, neither is skin due to high-velocity flow, Dq .

Two-Phase Flow Variables

Void fraction

$$\alpha = \frac{A_G}{A}$$

Hold-up

$$(1 - \alpha) = \frac{A_L}{A}$$

Velocity, u , u_G , u_L (m/s)

Mass flowrate, m , m_G , m_L (kg/s)

Volume flowrate, q , q_G , q_L (m³/s)

Mass quality

$$x = \frac{m_G}{m_G + m_L}$$

$$(1 - x) = \frac{m_L}{m_G + m_L}$$

Mass velocity or mass flux

$$G = \frac{m}{A} = \rho u = \frac{u}{v} \quad (\text{kg} / \text{s} \cdot \text{m}^2)$$

Density, ρ (kg/m³)

Specific volume, v (m³/kg)

Average (phase) velocities

$$u_G = \frac{m_G}{\rho_G A_G} = \frac{q_G}{A_G} = \frac{Gx}{\rho_G \alpha}$$

$$u_L = \frac{m_L}{\rho_L A_L} = \frac{q_L}{A_L} = \frac{G(1-x)}{\rho_L (1-\alpha)}$$

Volumetric flux or superficial velocity (note that A is used for all three definitions)

$$U = \frac{q}{A}$$

$$U_G = \frac{q_G}{A}$$

$$U_L = \frac{q_L}{A}$$

Slip ratio is defined as

$$K = \frac{u_G}{u_L}$$

It can be shown that

$$K = \left(\frac{x}{1-x} \right) \left(\frac{\rho_L}{\rho_G} \right) \left(\frac{1-\alpha}{\alpha} \right)$$

Density (exact value) of two-phase mixture is given by

$$\rho = \alpha \rho_G + (1-\alpha)\rho_L$$

It can be shown that

$$\alpha = \frac{x}{x + K(1-x) \frac{\rho_G}{\rho_L}}$$

If $K=1$

$$\alpha = \frac{x}{x + (1-x) \frac{\rho_G}{\rho_L}}$$

Two-phase homogeneous flow

$$u = u_G = u_L$$

$$K = \frac{u_G}{u_L} = 1$$

$$x = \frac{m_G}{m_G + m_L}$$

$$\alpha = \frac{q_G}{q_G + q_L}$$

$$x = \frac{\alpha}{\alpha + (1-\alpha) \frac{\rho_L}{\rho_G}}$$

$$\alpha = \frac{x}{x + (1-x) \frac{\rho_G}{\rho_L}}$$

$$-\frac{dp}{dz} = \frac{dp_f}{dz} + \frac{dp_a}{dz} + \frac{dp_g}{dz}$$

$$\frac{dp_f}{dz} = \frac{fG^2}{2\rho d}$$

$$\frac{dp_a}{dz} = \frac{d(G^2 / \rho)}{dz}$$

$$\frac{dp_g}{dz} = g\rho \sin \theta$$

Exact equation for mixture density

$$\rho = \alpha\rho_G + (1-\alpha)\rho_L$$

$$\text{Re} = \frac{Gd}{\mu}$$

Empirical equation for homogeneous mixture viscosity, commonly used in pressure drop calculations (exact equation not available)

$$\frac{1}{\mu} = \frac{x}{\mu_G} + \frac{(1-x)}{\mu_L}$$

Homogeneous model tends to under predict pressure drop, but can give reasonable results at high pressure and high mass flux, as in oil/gas wells, for example.

$$G = \rho u$$

$$\frac{fG^2}{2\rho d} = \frac{f\rho u^2}{2d}$$

Darcy-Weisbach equation for pressure drop in pipes

$$\Delta p = \frac{f}{2} \frac{L}{d} \rho u^2$$

Blasius equation for friction factor

$$f = \frac{0,3164}{\text{Re}^{0,25}}$$

used in two-phase flow for $2000 < \text{Re} < 100,000$.

Slip Ratio Equation

Derivation of the slip ratio equation

$$K = \left(\frac{x}{1-x} \right) \left(\frac{\rho_L}{\rho_G} \right) \left(\frac{1-\alpha}{\alpha} \right)$$

The slip ratio is defined as

$$K = \frac{u_G}{u_L}$$

We have

$$u_G = \frac{q_G}{A_G}$$

and

$$q_G = \frac{m_G}{\rho_G}$$

The same can be written for the liquid phase and we have

$$K = \frac{m_G}{\rho_G A_G} \frac{\rho_L A_L}{m_L}$$

We rewrite such that

$$K = \frac{\rho_L}{\rho_G} \left(\frac{m_G A_L}{m_L A_G} \right)$$

Definition of mass fraction is

$$x = \frac{m_G}{m_G + m_L}$$

which means that

$$\frac{m_G}{m_L} = \frac{x}{1-x}$$

Definition of void fraction is

$$\alpha = \frac{A_G}{A_G + A_L}$$

which means that

$$\frac{A_L}{A_G} = \frac{1-\alpha}{\alpha}$$

Substitution gives

$$K = \left(\frac{\rho_L}{\rho_G} \right) \left(\frac{x}{1-x} \right) \left(\frac{1-\alpha}{\alpha} \right)$$

or

$$\boxed{K = \left(\frac{x}{1-x} \right) \left(\frac{\rho_L}{\rho_G} \right) \left(\frac{1-\alpha}{\alpha} \right)}$$

Conversion Factors

Traditionally units	SI-equivalents	Useful info.
LENGTH mile (mi) yard (yd) foot (ft) inch (in)	M 1609.344 m # 0.9144 m # 0.3048 m # 0.0254 m #	grunnenhet 3 ft = 1 yd 12 in = 1 ft
VOLUME US-gallon (gal) UK-gallon (gal) API barrel (bbl) kubikkfot (cf)	m³ 0.00378541 m ³ 0.00454609 m ³ 0.158987 m ³ 0.0283167 m ³	1 bbl = 42 US gal 1 bbl ~ 5.62 cf
MASS pound (lbm) US-ton (ton) UK-ton (ton, tonne)	kg 0.45359 kg 907.185 kg 1016.05 kg	grunnenhet
TEMPERATURE Rankin (R) Celciusgrader (C) Fahrenheit (F)	Kelvin: K 5/9 K # K = C + 273 C = (F-32) · 5/9	grunnenhet R = F + 460
ENERGY, WORK kalori (cal) erg British Termal Unit (BTU) kilowatttime (kwh)	Joule: J 4.184 J # 10E-7 J 1055.06 J 3600 J	J = Nm
POWER hestekraft (elektrisk) (hk, hp) hestekraft (hydraulisk)	Watt: W 746 W # 746.043 W	W = J/s
FORCE dyn (dyn) kilopond, eller kilogramkraft (kp/kgf) poundforce (lbf)	Newton: N 10E-5 N # 9.80665 N 4.44822 N	N = kg m/s ² dyn = g cm/s ²
PRESSURE bar (bar) pound per square inch (psi) atmosfære (atm) mm kvikksølv (torr)	Pascal: Pa 105 Pa 6894.76 Pa 1.01325 bar # 133.322 Pa	Pa = N/m ² 1 bar ~ 14.5 psi 1 atm ~ 14.7 psi 1 atm ~ 1.01 bar
VISCOSITY poise (p) centipoise (cp) lbf/(ft ² /s)	Pa.s 10E-1 Pas # 10E-3 Pas # 4.78803 Pas	Pa.s = kg/s.m poise = dyn/cm ² s
DENSITY API-gravity (API) g/cm ³ lbm/US-gal lbm/UK-gal lbm/ft ³	kg/m³ kg/m ³ = (141.5)(1000)/(131.5 + API) 1000 kg/m ³ # 119.826 kg/m ³ 99.7763 kg/m ³ 16.0185 kg/m ³	
VOLUME FLOW liter pr. sek. (l/s) fat pr. dag (bbl/d) kubikkfot pr. dag (cf/d) US-gallon pr. minutt (gal/min)	m³/s 10E-3 m ³ /s 1.8401E-6 m ³ /s 3.2774E-7 m ³ /s 6.30903E-5 m ³ /s	

#: Exact values.

Composite Model of Geothermal Reservoirs

by
JON S. GUDMUNDSSON*
Petroleum Engineering Department
Stanford University
Stanford, CA

Introduction

The basic task of reservoir engineering is to quantify conceptual models of geothermal resources. Methods developed for this purpose range from empirical decline curves, through water influx modeling, to numerical simulation. Typically, a mathematical model is matched to the production history of a geothermal field, and then the model is used to predict the field's behavior with time. Reservoir engineering methods used in the geothermal industry are similar to those used in the petroleum industry and in groundwater hydrology. Nevertheless, there are reservoir engineering problems specific to the geothermal industry.

Geothermal resources are non-renewable, contrary to common belief outside the industry. When considering the non-renewable nature of geothermal resources, it is necessary to distinguish between a geothermal system and a geothermal reservoir. A geothermal system consists of the elements that give rise to geothermal resources: (1) rain in distant mountains that percolates deep into the earth and flows toward a reservoir, (2) movement of magma into the earth's crust and the formation of hot intrusions and dikes, and (3) zones of high permeability for hot water and steam to rise to drillable depths. Under favorable conditions these elements may provide the fluid, heat source, and rock permeability for a geothermal reservoir to exit. A geothermal reservoir is that part of the system that contains extractable heat. This heat must be extractable in industrial time rather than geologic time.

Geothermal reservoir modeling was recently reviewed by Grant (1983) and Bodvarsson and others (1985). A book on geothermal reservoir engineering is that of Grant and others (1982). Other relevant material is that of Ellis and Mahon (1977), Armstead (1978), Kestin (1980), Rybach and Muffler (1981), Edwards and others (1982), and Henley et al. (1984).

Heat-in-Place

In geothermal reservoirs the fluids constitute a small fraction of the total resource, because most of the energy is

in the rock. This can be illustrated by calculating the heat-in-place at typical reservoir conditions. Figure 1 shows the fraction of heat in steam vapor and liquid water for rock porosity from zero to 50 percent at a reservoir temperature of 250°C. The lines in Figure 1 represent steam and water filled rock. Reservoirs containing mixtures of liquid water and steam vapor will fall between the two lines, depending on the saturation.

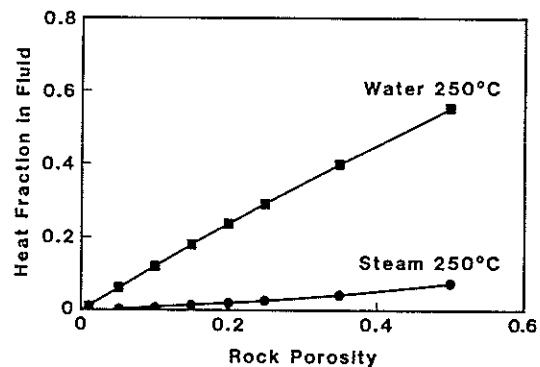


Figure 1. Fraction of heat in steam vapor and liquid water.

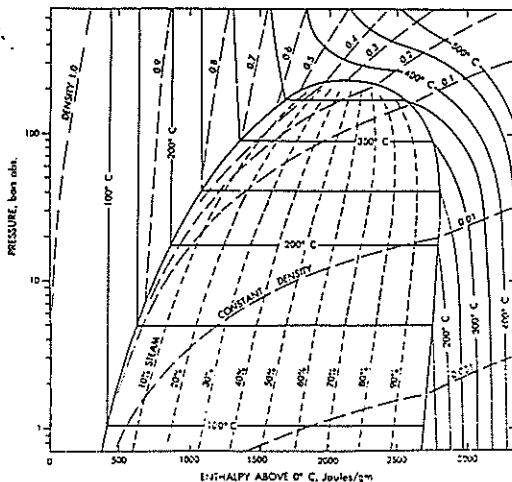
The bulk porosity of geothermal rock is typically in the range 5 to 15 percent. In such liquid filled rock at 250°C, the water contains 6 and 18 percent of the total heat, while the rock contains 94 and 82 percent. If the same rock is vapor filled, the steam contains 0.4 and 1.4 percent of the total heat, while the rock contains 99.6 and 98.6 percent of the heat or thermal energy.

The production of steam and water from a geothermal reservoir can be illustrated on a pressure-enthalpy diagram for pure water, shown in Figure 2 (Henley and others, 1984). The solid line is the saturation curve for water. Consider a steam-water mixture on the saturation curve at 250°C and 4 MPa pressure (40 bar abs.). Wells of this thermodynamic state could produce fluid in several ways. For example, production could be saturated liquid at an enthalpy of 1086 kJ/kg, or saturated at an enthalpy of 2800

*Permanent Address: Geothermal Division, Orkustofnun, Grensasvegur 9, Reykjavik, Iceland

kJ/kg, or any mixture of steam vapor and liquid water with an enthalpy ranging from that of steam and water.

Geothermal resources can be exploited by a variety of production mechanisms, ranging from isothermal fluid expansion to boiling throughout the reservoir. In the ideal case where a reservoir is isothermally drained of all its fluids, the energy recovery equals that contained in the steam or water. In the ideal case where the water in a liquid-dominated reservoir zone is allowed to evaporate to dry conditions, the energy recovery is much greater. This latter case will now be illustrated.



ENTHALPY ABOVE 0°C, Joules/gm

Figure 2. Pressure-enthalpy diagram for water.

Consider a unit volume of liquid filled rock at 250°C on the saturation curve (vapor pressure condition). When this reservoir volume is subjected to lower pressure the liquid water will evaporate to steam. The enthalpy of water at 250°C is 1086 kJ/kg and that of steam 2800 kJ/kg. This difference in enthalpy is the heat evaporation. It represents the energy required to change phase from liquid to vapor. This energy must be supplied by water itself or some other energy source. When water boils in a geothermal reservoir the formation rock provides the bulk of this energy — it does so by cooling. For rock porosity of 5 and 15 percent, all the fluid will have boiled after 25 and 90°C of cooling, respectively, assuming all the steam leaves the unit volume. Figure 3 shows the total energy recovery when liquid water boils from an initial temperature of 250°C. The total energy is that contained in the rock and water. For rock porosity of 5 percent an energy recovery of 13 percent is attained before the formation runs dry. When the porosity is 15 percent, about 50 percent of the energy is recovered. The energy recovery in this ideal case can be increased by fluid injection.

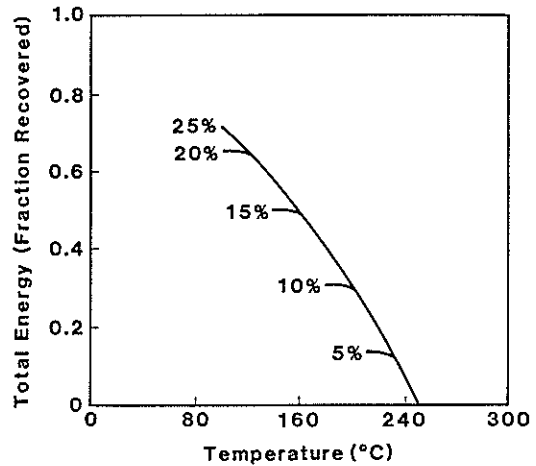


Figure 3. Total energy recovery on boiling.

Conceptual Models

Conceptual models are used in all stages of geothermal energy exploration and exploitation. Typically, exploration wells are located to delineate a resource, and production wells to intersect areas of high temperature and permeability. The location of these wells is in most cases based on a conceptual model of the reservoir. In turn, the data from wells are then used to confirm, or more likely, improve the conceptual model. The formulation of a conceptual model of a geothermal resource is an interdisciplinary task involving earth scientists and reservoir engineers alike. Several authors have reviewed the nature of geothermal systems and reservoirs and discussed generalized conceptual models; for example, White and others (1971), White (1973), Donaldson (1982), Donaldson and Grant (1982), Stefansson and Bjornsson (1982), and Sorey (1982).

The dominant mode of heat transfer near the surface of the earth is conduction. On average, the temperature increases with depth along a gradient of about 25°C/km, shown as curve A on Figure 4 (Combs and others, 1979). Higher conductive gradients occur in some geological provinces with relatively low thermal conductivity or relatively high crustal heat flow, as typified by curve B on Figure 4. High temperatures at shallow depths are commonly the result of convective flow. Convection may occur because of the heating and consequent thermal expansion of water at depth. Hot water of low density tends to rise and be replaced by cooler water of higher density. Convection increases temperatures in the upper part of a geothermal system, as shown by curves D and C in Figure 4. The temperature reversal of curve C may indicate a component of horizontal flow of water.

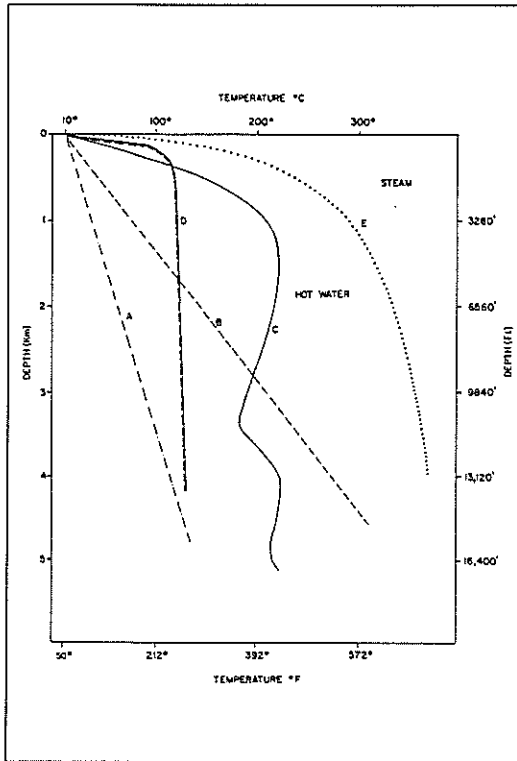


Figure 4. Typical temperature profiles.

Geothermal resources have often been classified according to their bulk or base temperature. For example, in Iceland the geothermal resources have traditionally been divided into high- and low-temperature areas (Bodvarsson, 1961, 1975). A geothermal resource is termed low-temperature if the reservoir temperature is below 150°C. These resources arise from the flow of water over long distances, up to 100 km, whereby the water becomes heated by the regional thermal gradient. Resources having temperatures above 150°C are termed high-temperature. However, they usually have a base temperature above 200°C. The high-temperature resources arise from the circulation of water near a magma intrusion and associated dikes. In the United States, geothermal resources have been divided into low-, moderate- and high-temperature reservoirs (Muffler, 1979; Reed, 1983). The temperature limits used are 90 and 150°C.

The maximum temperature in many geothermal systems follows the boiling point of water, shown as curve E in Figure 4. The position of the boiling point curve on a temperature-depth profile of a geothermal reservoir can vary according to the salinity and gas content of the subsurface fluids, and the depth of the local water table. The temperature gradient in many

geothermal reservoirs increases with depth until some characteristic base temperature of the system is attained. This behavior is shown in Figure 5 for the Svartsengi high-temperature field in Iceland.

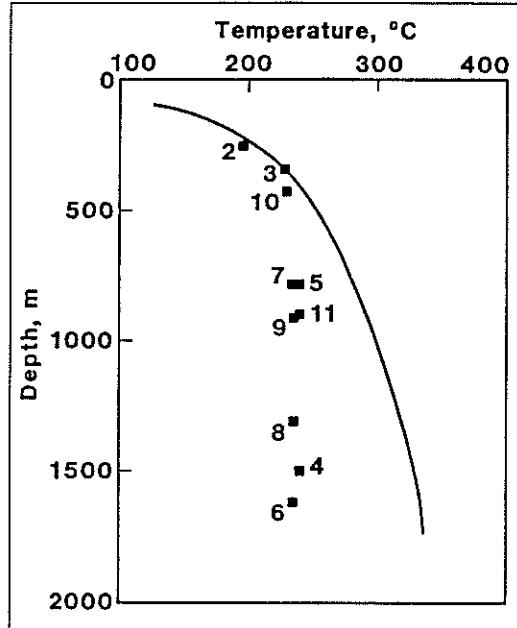


Figure 5. Temperature profile in Svartsengi field.

Geothermal reservoirs have traditionally been classified as either liquid-dominated or vapor-dominated (White and others, 1971). They differ in the fluid phase that dominates the pressure profile with depth. In liquid-dominated reservoirs the pressure increases hydrostatically with depth. Similarly, in vapor-dominated reservoirs the pressure increases vaporstatically with depth. Usually, this classification refers to the initial or natural state of a geothermal reservoir. As more and more geothermal fields have been discovered and developed, however, it has become clear that a single reservoir can have regions under both liquid- and vapor-dominated conditions. During development the size of the different regions changes with time as more and more fluids are produced.

Steam vapor and liquid water are thought to coexist in vapor-dominated zones and reservoirs. The main observation supporting this statement is that the amounts of steam produced at The Geysers in California and Larderello in Italy exceeds the steam vapor content of the known reservoir volume (Economides and Miller, 1985). A vapor-dominated zone can be thought of as containing steam vapor in the fractures of the reservoir, while liquid water resides in the porous rock matrix. The liquid water saturation is low and steam vapor is the flowing phase. The temperature within a vapor-dominated zone is usually uniform, suggesting long-term circulation of steam and

water within the reservoir. A plausible model consists of steam vapor rising within the fractures, condensing near the top of the reservoir, and then draining as liquid water through the rock matrix.

A vapor-dominated zone is likely to be surrounded by liquid water saturated formations at the top and sides. Some of this water may enter the hot zone or reservoir when steam is produced and pressure falls. A distinction should be made between the physical and chemical processes giving rise to vapor-dominated zones and reservoirs over geologic time, and the processes taking place over industrial time; that is, the time it takes to deplete a geothermal reservoir.

Vapor- and liquid-dominated reservoirs are recognized by the different densities dominating their pressure profile with depth. This difference has been the main basis for their classification. However, they have an equally important common feature, namely the temperature profile with depth. The temperature profile in a typical well at The Geysers is similar in shape to that shown in Figure 5, which is measured in a liquid-dominated reservoir. Their common feature is the near constant temperature within the bulk of the reservoir. This uniform temperature profile is established because there is good fluid communication between different parts of the reservoir; that is, high permeability in all directions. Both types of reservoirs are dynamic. Steam vapor rises and liquid condensate drains down in vapor-dominated zones, while liquid water convects from great depths to near the surface in liquid-dominated zones.

Boiling Conditions

The temperature profile in wells in liquid-dominated reservoirs is often said to be on the boiling point for depth curve in Figure 4. Two aspects of this observation need to be considered. First, the water in the wells may follow the boiling point curve while the reservoir does not. This situation can arise when there is interzonal flow near the bottom of a well that heats the water column by rising steam bubbles, for example. That is, the temperature profile measured in a static wellbore need not be the same as in the reservoir. Second, the temperature profile in the reservoir follows the boiling point curve, which may or may not be apparent from wellbore measurements. This complicates the interpretation of temperature and pressure profiles in static wells (Grant and others, 1983). It has been recognized for some time that the true reservoir pressure and temperature are shown at only one depth in many geothermal wells. This depth is where the main feedzone fracture of the wells is located; that is, where the wellbore is connected to the reservoir. Therefore, careful analysis of downhole measurements is called for to estimate the true reservoir temperature and pressure. The temperature values in Figure 5, for example, are measured at the depth of the main feedzone fracture of the wells.

It is necessary to extend the classification of geothermal zones and reservoirs to include conditions where the formation temperature follows the boiling point for depth curve. For the purpose of the present paper, such

conditions are called boiling-dominated, partly to conform to the liquid- and vapor-dominated classification. Similar reservoir conditions have been studied by Grant (1977), Whittome and Smith (1979), and Stefansson and Steingrimssson (1980). Figure 6 shows downhole pressure and temperature measurement in wells in the Krafla reservoir in Iceland (Stefansson and Steingrimssson, 1980). The shown values are measured near the main feedzone of the wells, so they represent reservoir conditions. These and other data from the field indicate that most of the reservoir formation was near the boiling point curve in its natural state (Stefansson 1980).

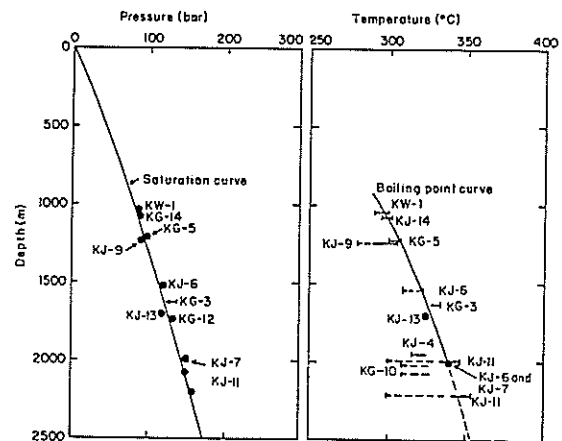


Figure 6. Temperature and pressure measurements in Krafla field.

Boiling-dominated zones are often called two-phase reservoirs. In the natural state the pressure profile with depth in both liquid- and boiling-dominated zones is hydrostatic. However, when these two types of reservoir zones are subjected to fluid production, they will respond differently. The main difference is that wells in liquid-dominated zones will have all-liquid-feed, until pressures are reduced to saturation values, while wells in boiling-dominated zones will have two-phase-feed. Two-phase feed implies that liquid and steam flow into the well. Liquid water at the boiling point will start to boil immediately when the confining (surrounding) pressure is lowered due to production. A boiling-dominated zone may arise in the natural state for several reasons. A likely reason is limited fluid communication within the reservoir - at least much less than in a liquid-dominated zone. This would suggest that boiling-dominated zones are likely to have low permeability, so wells drilled into

such zones will have low flowrates. However, the specific enthalpy of the fluids produced will be high, which to some extent may compensate for the low flowrates. Another reason could be high gas content of the geothermal fluid, which would lead to boiling at great depth.

Composite Resource

A composite diagram of a typical geothermal resource area is shown in Figure 7. The emphasis of this diagram is on the mode of fluid discharge and production from geothermal reservoirs. It represents a conceptual model of a reservoir having all types of formation conditions: vapor-, liquid- and boiling-dominated zones. The following descriptions refer to the diagram (the wells shown can be thought of as wellfields):

Hot springs. Geothermal resources are commonly manifested at the surface of the earth by thermal springs. Hot water from the main reservoir flows through a fracture up to the surface, perhaps mixing with local groundwater. Hot springs are likely to be found at low elevations in geothermal resource areas. It is common for hot springs to disappear when reservoir pressure falls due to fluid production.

Hot water wells. A well drilled into a fracture feeding hot springs will produce hot water, that is often used in direct use applications. The chemistry of the fluids produced can be indicative of the hotter fluids deep in the reservoir.

Two-phase wells with liquid feed. A well drilled into a liquid-dominated zone will have a liquid only feedzone. As this water flows up to the wellbore it will start to flash and a two-phase mixture is produced at the wellhead.

Fumaroles and mud pots. Geothermal resources are often manifested at the surface of the earth by steam related phenomena such as fumaroles and mud pots, also solfataras. Steam flows from the natural steam cap or two-phase zone of the main reservoir through a fracture to the surface, in some cases mixing with local groundwater. Fumaroles are likely to be found at high elevations in geothermal resource areas.

Steam wells. Wells drilled into vapor-dominated zones will produce saturated or perhaps superheated steam. Vapor-dominated zones are found to exist in the natural state at the top of geothermal formations that are otherwise liquid filled. As fluid is produced from liquid- and boiling-dominated reservoirs, such steam zones will grow in size. A vapor-dominated reservoir can be thought of as arising from a liquid-dominated formation, where the liquid water has been expelled from the fractures by boiling.

Two-phase wells with two-phase feed. In the natural state the reservoir formation surrounding this kind of a well was boiling-dominated. Two-phase conditions form quickly and a mixture of steam and water flows into the wellbore. The flowrate and enthalpy of such wells are likely to change with time.

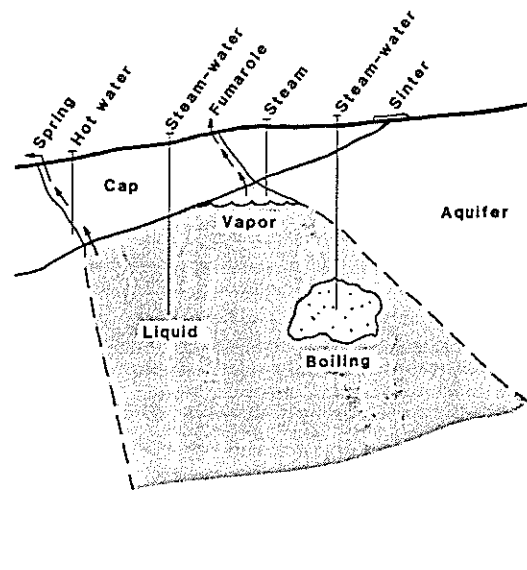


Figure 7. Composite geothermal resource area.

Sinter deposits. When liquid water from a reservoir with a base temperature of 180°C and higher flows to the surface, silica will be deposited. Lower temperature waters will form travertine deposits (White, 1973). Combined with other surface manifestations such as thermal springs and fumaroles, therefore, sinter deposits can indicate the likely reservoir temperature in fields where no drilling has taken place.

Capping structure. Almost all geothermal resources are contained under some capping structure, which nevertheless may have faults and fractures that connect the reservoir to the surface. This structure is of low permeability, typically as a result of hydrothermal alteration of the near surface rocks.

Surrounding aquifers. It has been found that geothermal reservoirs are in fluid communication with warm and cold aquifers surrounding the resource area. As pressure decreases upon fluid production, the surrounding waters will encroach into the hot reservoir.

Material-Balance/Water-Influx

Techniques based on material balance have long been regarded as one of the basic tools of reservoir engineers for interpreting and predicting reservoir performance. These techniques are also called lumped-parameter modeling. The assumption is made that a geothermal reservoir will

respond to production as one unit with appropriate fluxes of fluid and heat specified at its boundaries. The reservoir and surrounding aquifers are assumed to have some average fluid and rock properties. Lumped-parameter modeling has successfully described the performance of many developed geothermal fields. Perhaps the major reason for this is that only fields with high permeability have been developed. Such fields tend to have uniform rock and fluid properties and high overall deliverability.

The first application of the material balance technique to a geothermal reservoir is that of Whiting and Ramey (1969), who studied the Wairakei liquid-dominated field in New Zealand. A study on a vapor-dominated field is that of Brigham and Neri (1980), who modeled the Larderello reservoir in Italy. Other lumped-parameter studies are those of Grant (1977), Sorey and Fradkin (1979), Castaner and others (1980), Fradkin and others (1981), Dee and Brigham (1985), and Gudmundsson and Olsen (1985).

A geothermal reservoir can be thought of as a large volume of fluid saturated rock at high temperature surrounded by warm and cold aquifers (see Figure 7). With fluid production from the reservoir, water from the sur-

rounding aquifers will flow (encroach) into the reservoir. How this happens and at what rate is likely to depend on the system geometry, and the flow resistance across the reservoir-aquifer boundary. The use of water influx methods in geothermal reservoir engineering has been reviewed by Olsen (1984).

Several options are available in the modeling of aquifers surrounding geothermal reservoirs. The geometry can be radial or linear; the fluid flow across the reservoir-aquifer boundary can be at constant rate or pressure; the outside boundary of the aquifer can be at a finite or infinite distance. Furthermore, the flow of aquifer water into the reservoir can be steady, pseudo-steady, or unsteady state. Craft and Hawkins (1959) and Dake (1978) provide additional details.

Water influx modeling of the Svartsengi field in Iceland has been reported by Gudmundsson and Olsen (1975). It is an example of a lumped-parameter model applied to a liquid-dominated system where the hot reservoir and surrounding aquifers are treated as two distinct elements. Figures 8 to 10, show the correlation between the rate of production and reservoir drawdown

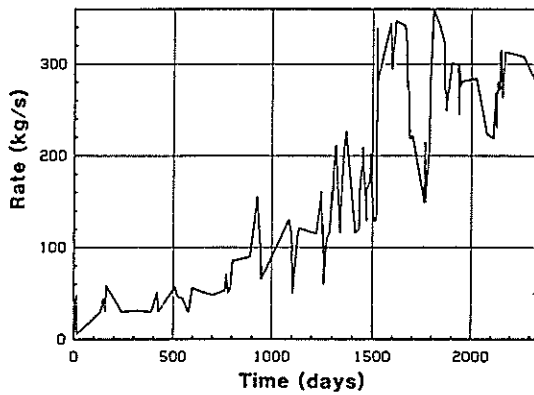


Figure 8. Rate of production with time in Svartsengi field.

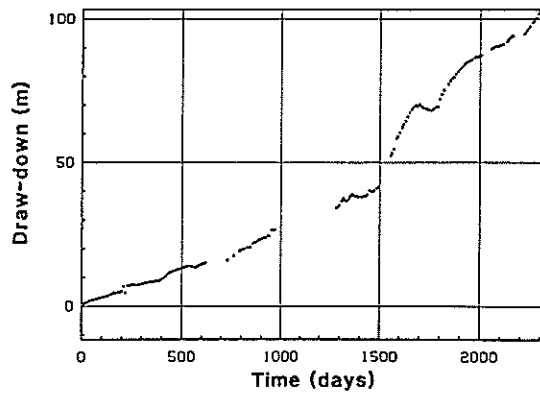


Figure 9. Water level drawdown with time in Svartsengi field.

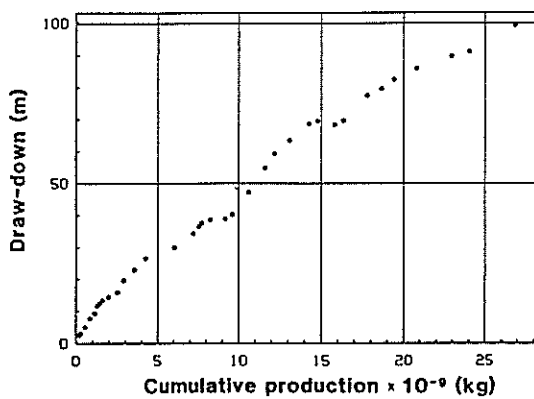


Figure 10. Water level drawdown with cumulative mass production in Svartsengi field.

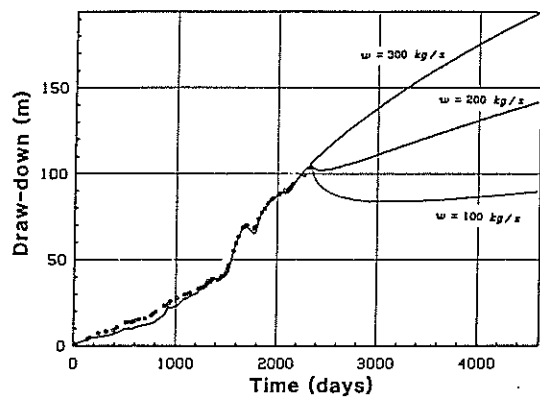


Figure 11. Water influx model match and prediction for drawdown with time in Svartsengi field.

in the Svartsengi field. For example, when the rate (w) was decreased from above 300 kg/s to below 200 kg/s between 1600 and 1700 days, the drawdown was not only halted, but reverted for some time; this behavior demonstrates the effect of water influx. One of the water influx models used by Gudmundsson and Olsen (1985) was the Hurst (1958) simplified method. The Svartsengi data were matched and the field behavior predicted with time, assuming three constant production rates: 100 kg/s, 200 kg/s, and 300 kg/s. The reservoir-aquifer geometry was taken as linear, and the outer boundary of the aquifer was assumed at infinite distance. The matched and predicted results are shown in Figure 11. Note that the field behavior was predicted into the future for the same length of time as there are production data.

Summary

- (a) Conceptual models are used in all stages of geothermal exploration and exploitation. The basic task of reservoir engineering is to quantify conceptual models of geothermal resources. Reservoir engineering models are of three main types: empirical decline, lumped-parameter, and numerical simulation.
- (b) The heat content of steam vapor and liquid water in a typical geothermal reservoir is much less than that of the solid rock. In a reservoir at 250°C and with a formation porosity of 5 percent, the fluid contains 6 percent of the total heat content when the rock is liquid-filled, and 0.4 percent when it is vapor-filled. If a liquid-filled reservoir at 250°C (and 5 percent porosity) is allowed to boil-off the water, about 13 percent of the total heat content of the formation is recovered; that is, before the rock becomes dry.
- (c) Geothermal reservoir zones have traditionally been classified as vapor-dominated and liquid-dominated; they differ in the fluid phase that determines the reservoir pressure profile with depth. Typically such reservoir zones are observed to have a near constant temperature profile with depth. Most liquid-dominated reservoirs have steam caps that increase in size with fluid production. In some liquid-dominated reservoirs the temperature increases along the boiling point curve throughout. Such reservoirs become two-phase immediately upon production.
- (d) Surface manifestations of geothermal resources include: hot springs, fumaroles, sinter deposits, mud pots, and in some cases geysers. Wells drilled into geothermal reservoirs can produce hot water, a steam-water mixture, or steam only. Fluid producing zones in geothermal reservoirs can be vapor-, liquid-, or boiling-dominated. Geothermal reservoirs have capping structures, typically, and are surrounded by hot and cold water aquifers.
- (e) Lumped-parameter modeling (material balance coupled with water influx) is used to match geothermal reservoir production data, and to predict future pressure decline. The future should not be predicted for a longer period than there is production history.

The main use of such modeling to field development is to estimate when make-up wells need to be drilled, and what effect an increased fluid production rate (additional power unit) would have on reservoir drawdown. Lumped-parameter modeling can provide reliable answers to such questions early on in the development of geothermal fields. □

References

- Armstead, H.C.H., (1978). *Geothermal Energy: Its Past, Present and Future Contributions to the Energy Needs of Man*, E.&F.N. Spon, London.
- Bodvarsson, G.S., (1961). *Physical Characteristics of Natural Heat Resources in Iceland*, *Jokull*, 11, 29-38.
- Bodvarsson, G.S., (1975). *Estimates of the Geothermal Resources of Iceland*, Proc., Second UN Symp. Development Uses Geoth. Resources, San Francisco, CA, 33-35.
- Bodvarsson, G.S., Pruess, K. and Lippmann, M.J., (1985). *Modeling of Geothermal Systems*, SPE Paper 13613, Society of Petroleum Engineers, California Regional Meeting, Bakersfield, CA.
- Brigham, W.E. and Neri, G., (1980). *Depletion Model for the Gabbro Zone (Northern Part of Lardello Field)*, Proc., Second DOE-ENEL Workshop Cooperative Research Geothermal Energy, Berkeley, CA 434-463.
- Castanier, L.M., Sanyal, S.K. and Brigham, W.E., (1980). *A Practical Analytical Model for Geothermal Reservoir Simulation*, Paper SPE 8887, SPE California Regional Meeting, Los Angeles, CA.
- Combs, J., Applegate, J.A., Fournier, R.O., Swanberg, C.A. and Neilson, D., (1979). *Exploration, Confirmation and Evaluation of the Resource*, Direct Utilization of Geothermal Energy: A Technical Handbook, D.N. Anderson and J.W. Lund (eds.), Geothermal Resources Council, Special Report 7, 2.1-2.16.
- Craft, B.C. and Hawkins, M.F., (1959). *Applied Reservoir Engineering*, Prentice-Hall, Inc., Englewood Cliffs, NJ.
- Dake, L.P., (1978). *Fundamentals of Reservoir Engineering*, Elsevier, Amsterdam.
- Dee, J.F. and Brigham, W.E., (1985). *A Reservoir Engineering Analysis of a Vapor-Dominated Geothermal Field*, Proc., Tenth Workshop Geothermal Reservoir Engineering, SGP-TR-84, Stanford University, Stanford, CA, 97-103.
- Donaldson, I.G., (1982). *Heat and Mass Circulation in Geothermal Systems*, *Ann. Rev. Earth Planet. Sci.*, 10, 377-395.
- Donaldson, I.G. and Grant, M.A., (1981). *Heat Extraction from Geothermal Reservoirs*, *Geothermal Systems: Principles and Case Histories*, L. Rybach and L.J.P. Muffler (eds.), John Wiley & Sons, Chichester, England, 145-179.
- Economides, M.J. and Miller, F.G., (1985). *The Effects of Adsorption Phenomena in the Evaluation of Vapor-Dominated Geothermal Reservoirs*, *Geothermics*, 14 (1), 3-27.
- Edwards, L.M., Chilingar, G.V., Rieke, H.H. and Fertl, W.H. (eds), (1982). *Handbook of Geothermal Energy*, Gulf Publishing Company, Houston, TX.
- Ellis, A.J. and Mahon, W.A.J., (1977). *Chemistry and Geothermal Systems*, Academic Press, New York, N.Y.
- Fradkin, L.J., Sorey, M.J. and McNabb, A., (1981). *On Identification and Validation of Some Geothermal Models*, *Water Resources Research*, 17(4), 929-936.
- Grant, M.S., (1977). *Broadlands: A Gas-Dominated Field*, *Geothermics*, 6 (1), 9-29.
- Grant, M.A., (1983). *Geothermal Reservoir Modeling*, *Geothermics*, 12 (4), 251-63.
- Grant, M.A., Donaldson, I.G. and Bixley, P.F., (1983). *Geothermal Reservoir Engineering*, Academic Press, New York.
- Grant, M.A., Bixley, P.F. and Donaldson, I.G., (1983). *Internal Flows in Geothermal Wells: Their Identification and Effect on the Wellbore Temperature and Pressure Profiles*, *Soc. Pet. Eng. J.*, 168-176.
- Gudmundsson, J.S. and Olsen, G., (1985). *Water Influx Modeling of Svartsengi Geothermal Field, Iceland*, SPE Paper 13615, Society of Petroleum Engineers, California Regional Meeting, Bakersfield, CA.

- Henley, R.W., Truesdell, A.H. and Barton, P.B., (1984). *Fluid-Mineral Equilibria in Hydrothermal Systems*, Economic Geology Publishing Company, El Paso, TX.
- Hurst, W., (1958). *The Simplification of the Material Balance Formulas by the Laplace Transformation*, Trans. AIME, 213, 292-303.
- Kestin, J. (ed), (1980). *Sourcebook on the Production of Electricity from Geothermal Energy*, US Department of Energy, DOE/RA/4051-1.
- Muffler, L.J.P. (ed), (1979). *Assessment of Geothermal Resources of the United States 1978*, US Geological Survey, Circular 790, Menlo Park, CA.
- Olsen, G., (1984). *Depletion Modeling of Liquid-Dominated Geothermal Reservoirs*, SGP-TR-80, Stanford Geothermal Program, Stanford, CA.
- Reed, M.J. (ed), (1983). *Assessment of Low-Temperature Geothermal Resources of the United States 1982*, US Geological Survey, Circular 892, Menlo Park, CA.
- Rybach, L. and Muffler, L.J.P. (eds), (1981). *Geothermal Systems: Principles and Case Histories*, John Wiley & Sons, Chichester, England.
- Sorey, M.L., (1982). *Geothermal Reservoirs in Hydrothermal Convection Systems*, Proc., Eighth Workshop Geothermal Reservoir Engineering, SGP-TR-60, Stanford University, Stanford, CA 5-17.
- Sorey, M.L. and Fradkin, L.J., (1979). *Validation and Comparison of Different Models of the Wairakei Geothermal Reservoir*, Proc., Fifth Workshop Geothermal Reservoir Engineering, Stanford University, Stanford, CA, 215-220.
- Stefansson, V., (1980). *The Krafla Geothermal Field, Northeast Iceland*, Geothermal Systems: Principles and Case Histories, L. Rybach and L.J.P. Muffler (eds), John Wiley & Sons, Chichester, England, 273-294.
- Stefansson, V. and Bjornsson, S., (1982). *Physical Aspects of Hydrothermal Systems*, Continental and Oceanic Rifts, G. Palmason (ed), AGU Geodynamic Series, 8, 123-145.
- Stefansson, V. and Steingrimsen, B., (1980). *Production Characteristics of Wells Tapping Two Phase Reservoir at Krafla and Namafull*, Proc., Sixth Workshop Geothermal Reservoir Engineering, SGP-TR-50, Stanford, CA, 49-59.
- White, D.E., (1973). *Characteristics of Geothermal Resources*, Geothermal Energy, P. Kruger and C. Otte (eds), Stanford University Press, Stanford, CA, 69-94.
- White, D.E., Muffler, L.J.P. and Truesdell, A.H., (1971). *Vapor-Dominated Hydrothermal Systems Compared with Hot-Water Systems*, Economic Geology, 66, 75-97.
- Whiting, R.L. and Ramey, H.J. Jr., (1969). *Application of Material and Energy Balances to Geothermal Steam Production*, J. Pet. Tech., 893-900.
- Whittome, A.J. and Smith, E.W., (1979). *A Model of the Tongonan Geothermal Field*, Proc., First New Zealand Geothermal Workshop, Auckland, 141-147.

Two-Phase Wells

by
JON S. GUDMUNDSSON*
Petroleum Engineering Department
Stanford University
Stanford, CA

Introduction

The output of two-phase geothermal wells consists of steam vapor and liquid water at some wellhead pressure. Typically, this two-phase mixture is piped to a separator to produce steam for electric power generation. The liquid water separated from the steam is disposed of at the surface or injected back into the reservoir. The rate and pressure of the steam produced by individual wells is an important parameter in the feasibility of geothermal electric power developments.

A paper on the output behavior of two-phase geothermal wells is that of James (1970). It deals with the measurement of flow and enthalpy, the maximum flow and wellhead pressure of wells in liquid-dominated reservoirs, the effect of casing diameter on output, and the realization that water flows into geothermal wells through fractures. These technical issues remain of great importance in the geothermal industry. Recently James, (1983) considered the effect of long term production on the output curve of two-phase wells.

Studies of two-phase flow in geothermal wellbores are those of Gould (1974) and Nathenson (1974). Both provide a good introduction to two-phase wellbore flow. The Gould (1974) study was based on methods developed in the petroleum industry, and the applications considered were wellbore deposition and deliverability calculations. The Nathenson (1974) study considered homogeneous wellbore flow and coupled it to porous media flow in the reservoir. The problems investigated by Nathenson (1974) were deliverability and wellbore deposition. He also considered the effect of reservoir permeability on output and the useful energy (available energy) produced by typical wells for electric power generation. Upadhyay and others (1977) developed a wellbore simulator and compared calculated and observed pressure drops in two-phase geothermal wells. Several similar studies have since been carried out, including that of Gudmundsson and others (1984). Typical uses of wellbore models in the development of geothermal resources have been reported by Miller and Harrison (1985).

Typical Wells

Geothermal wells have flowrates that are an order of magnitude greater than the flow of most oil and gas wells.

*Permanent address: Geothermal Division, Orkustofnun, Grensasvegur 9, Reykjavik, Iceland.

A typical geothermal well produces at steam/water rates sufficient to generate about 5 MW of electrical power. This assumption can be verified by using wellfield data made available to the Geothermal Resources Council for the 1985 International Symposium on Geothermal Energy. The average electric power capacity of wells in 12 fields worldwide are shown in Table 1 and Figure 1. Fields having fewer than 5 production wells were omitted, so were all wellfield data from Japan. It seems that geothermal wells in Japan have noticeably less output than wells elsewhere in the world, either because the Japanese fields were overexploited, or perhaps many of the wells are used for injection purposes. The data reported to the Geothermal Resources Council were total mass flowrate and mixture enthalpy for all wells drilled in a given geothermal field. Non-productive wells and injection wells were included when adding the total number of wells drilled in a field. The average capacity of these wells was estimated by assuming that the thermal power produced could be converted into electric power with an efficiency of 10 percent.

Table 1. Average electric power capacity of wells in geothermal fields worldwide.

Field, Country	Wells	Capacity (MWe)
Svartsengi, Iceland	11	10.4
Mokai, New Zealand	5	10.0
Tongonan, Philippines	52	7.5
Miravalles, Costa Rica	5	6.6
Broadlands, New Zealand	45	5.8
Tiwi, Philippines	90	5.3
Palinpinon, Philippines	51	4.6
Bacon-Manito, Philippines	19	4.5
Kizildere, Turkey	16	4.4
Mak-Ban, Philippines	83	4.2
Wairakei, New Zealand	120	3.0
Krafia, Iceland	24	1.6
Total	521	---

Two-phase geothermal wells can have a liquid only or a steam-water feedzone. When liquid water flows into a geothermal well, the water will remain liquid up the wellbore until reaching a depth where the pressure is the same as the saturation pressure. At this depth the liquid water will start to flash to form steam. It will continue to flash until reaching the wellhead, surface pipeline, and eventually the steam-water separator. If the flowrate and total mixture enthalpy of such a

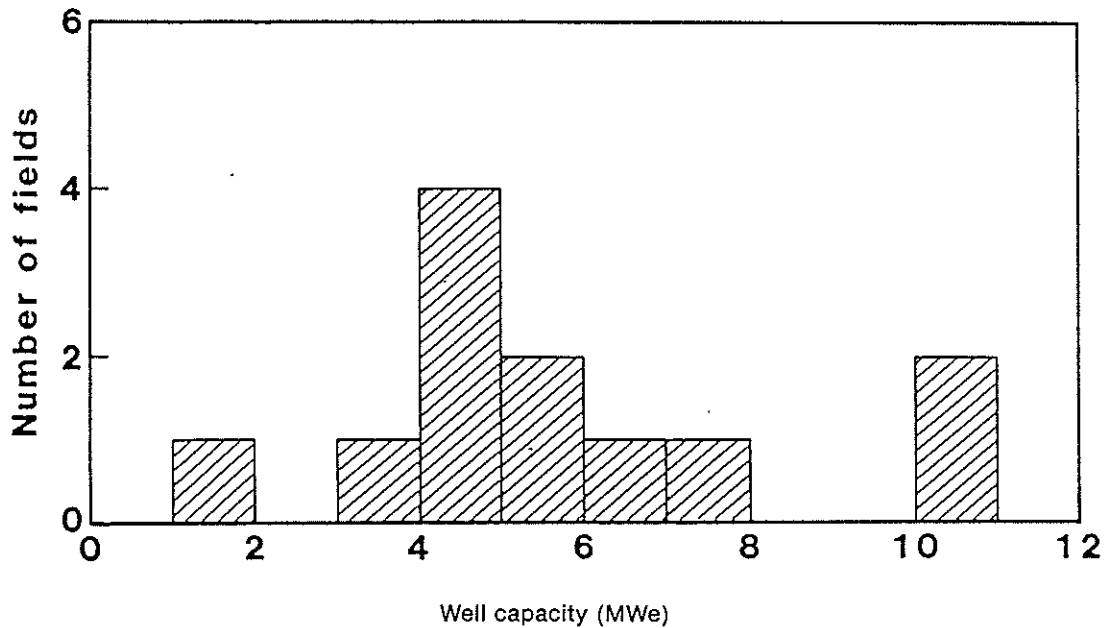


Figure 1. Average capacity of wells in geothermal fields worldwide.

well were measured, the results could be plotted as shown in Figure 2. This figure shows an output test on well 1 in the Miravalles field in Costa Rica (Gudmundsson and others, 1984). The total mixture flowrate and enthalpy were measured at several wellhead pressures. The mass flowrate shows the typical behavior of two-phase wells that have a liquid only feed. At low wellhead pressures the flowrate is the highest, and as the wellhead pressure increases the flowrate becomes less. The mixture enthalpy, however, remains constant. Although the measured enthalpy ranges from 970 to 990 kJ/kg, the values must be interpreted as resulting from the same liquid feed. Experience has shown that under the best of conditions the enthalpy of two-phase geothermal mixtures cannot be measured more accurately than 20 kJ/kg above or below the true value (Grant and others, 1982). Liquid water at 225 to 230°C has the enthalpy values measured. That is, the water that flows into well 1 in Miravalles must be in this temperature range.

The situation where a two-phase mixture flows into the wellbore is different from the case where the feed is liquid only. The two-phase feed can result from several reservoir-wellbore flow conditions: it could be liquid water that flashes as it flows toward the wellbore, it could be that the overall fluid state in the reservoir is two-phase or, the well could have two feedzones one of which has liquid feed and the other steam. For whatever reason a geothermal well receives a mixture of steam and water, the end result is that the mixture enthalpy may now depend on wellhead pressure. This behavior is shown in Figure 3 for well 2 in the Los Azufres field in Mexico (Molinar, 1985). The mass flowrate decreases with increasing wellhead

pressure just as in Figure 2. However, instead of the mixture enthalpy remaining constant, it now decreases with increasing wellhead pressure. Another example of this kind of behavior has been presented by Menzies and

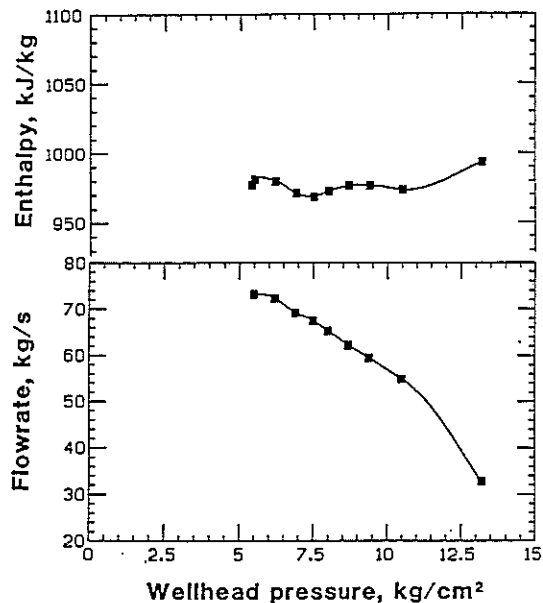


Figure 2. Output curve and enthalpy of well 1 in Miravalles field, Costa Rica.

others (1982) for well 403 in the Tongonan field in the Philippines.

The output curve of a geothermal well shows the flowrate, enthalpy, and wellhead pressure at the time of measurement. After a few months or years of production the downhole conditions are likely to change due to reservoir drawdown. It follows that the output curve of geothermal wells will change with time. The rate of change will depend on the overall reservoir-wellbore system. Examples of this behavior have been reported by Stefansson and Steingrímsson (1980) for well 11 in the Namafjall field and well 12 in the Krafla field in Iceland, and by Grant and Glover (1984) for well 21 in the Broadlands field in New Zealand. The first year output behavior of well 12 in the Krafla field is shown in Figure 4. It shows that after one week of discharge the well was producing steam only. Although not shown on the figure, the steam flowrate was found to be independent of wellhead pressure. This behavior indicates that the rate of flow was determined by the steam pressure drop through the reservoir.

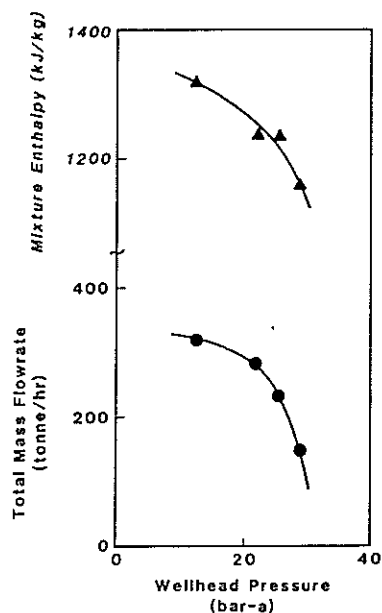


Figure 3. Output curve and enthalpy of well 2 in Los Azufres field, Mexico.

Casing Design

The output of two-phase geothermal wells is determined primarily by the feedzone permeability, fluid enthalpy, and wellbore diameter. Other factors include fluid chemistry, and well depth and roughness. For a given geothermal resource, therefore, the casing design is the only factor that can be optimized. It was demonstrated by Budd (1973) that the well diameter and feedzone depth in vapor-dominated reservoirs determines the rate of steam

flow to the surface. In the case of liquid-dominated reservoirs, however, this output behavior has not been demonstrated in the field until more recently (Gudmundsson and others, 1981).

The Svartsengi field in Iceland is a typical liquid-dominated reservoir containing water at 235-240°C. The wells have liquid feed and flashing starts up the wellbore at depths of 200-400 m. It was found that calcium carbonate deposits formed in the wellbore where the flashing started. These deposits have to be cleaned out by drilling (reaming) about once per year. The early deep wells in Svartsengi had a 9- $\frac{1}{2}$ in. production casing down to about 600 m depth. To try to cut down on the frequency of wellbore cleaning, it was decided to increase the size of the production casing of all new wells to 13- $\frac{1}{2}$ in. The total depth of these wells is in the range 1000-1600 m. At standard operating conditions the output of the 9- $\frac{1}{2}$ in. wells is about 60 kg/s of steam-water mixture. However, the 13- $\frac{1}{2}$ in. wells produce at least double that amount. It seems that the increase in flow is directly proportional to the cross-sectional area of the wellbore. The output curves of the 9- $\frac{1}{2}$ in. and 13- $\frac{1}{2}$ in. wells in the Svartsengi field are shown in Figure 5. The wells are closely spaced at about 200 m and produce from similar depths. The Svartsengi reservoir must be highly permeable for the wellbore to have so much effect on the output.

The wells in the Svartsengi field have a production casing of a uniform diameter, either 9- $\frac{1}{2}$ in. or 13- $\frac{1}{2}$ in. At greater depth the wells have a 7 or a 9- $\frac{1}{2}$ in. slotted liner, respectively. Geothermal wells can also be of stepped design where several production casing diameters are used in the same well. Bilicki and others (1982) studied the theoretical effect of stepped casing design on the output of a typical well at Brawley in the Imperial Valley, U.S.A. Their casing designs are shown in Figure 6. The reservoir

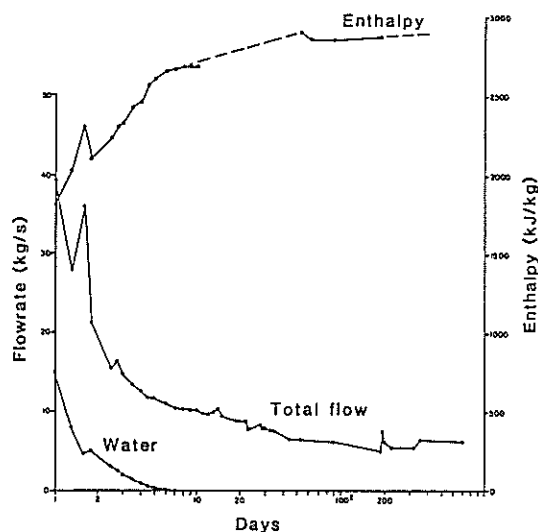


Figure 4. First year of flowrate and enthalpy of well 12 in Krafla field, Iceland.

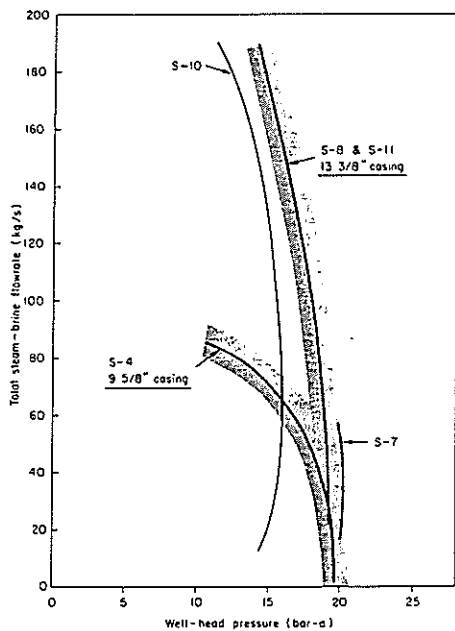


Figure 5. Output curves of wells in Svartsengi field, Iceland.

temperature was assumed 250°C, the total dissolved solids 15 wt. %, the reservoir pressure 24.2 MPa, and the laminar flow productivity index 0.0182 kg/s.MPa. The uniform wellbore diameter shown corresponds to 7-5/8 in. casing, and the two larger diameters in the stepped well correspond most likely to 11-3/4 in. and 20 in. casing. The calculated output curves of the two wells are shown in Figure 7. They show that if wells were operated at a wellhead pressure of 0.9 MPa (900 kPa), the stepped well is capable of delivering nearly 2.5 times as much flow as the uniform well.

Discharge Analysis

The output curve of a two-phase geothermal wells with a liquid feed can be estimated using the discharge analysis method presented by Gudmundsson (1984). The discharge analysis method is based on three key elements. The first of these is having a wellbore simulator for two-phase geothermal wells. This makes it possible to calculate down-hole flowing pressures corresponding to measured wellhead conditions. The simulator must have the capability to start the calculations from both the wellhead and wellbottom.

The second key element is the concept of inflow performance; that is, the flow of fluid from the reservoir and into the wellbore. If the flow is laminar (Darcy flow) the well known oil and gas industry productivity index can be used:

$$P.I. = \frac{w}{\bar{p} - p_{wf}}$$

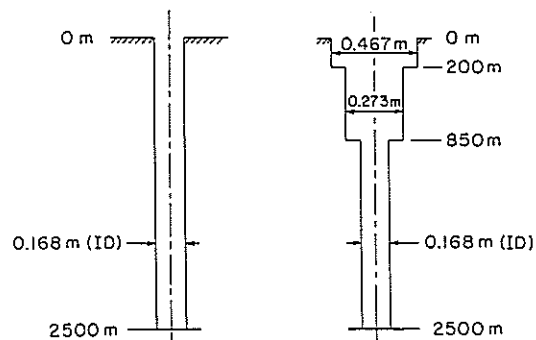


Figure 6. Casing design for uniform and stepped wells in a Brawley-type reservoir.

where w represents the total flowrate and \bar{p} and p_{wf} the average reservoir pressure (static) and the well flowing pressure, respectively. The productivity index is assumed to stay constant not only with flowrate but also with time. However, the average reservoir pressure can change with time. The wells are assumed to have reached steady flowing conditions when measured. Also, the method refers to the well discharge curve at the end of the output measurement used.

If the rate of flow from the reservoir and into the wellbore is large, or the feedzone fracture is narrow, the flow may become turbulent. In this case the productivity index should not be used. Other inflow functions are more appropriate when the flow is partly or fully turbulent. For example the two constant equation (Nind, 1981):

$$\Delta p = \alpha \cdot w^{\frac{1}{2}} + \beta \cdot w^2$$

where the two terms on the right hand side represent the laminar and turbulent contribution to the pressure drop, respectively. The pressure drop Δp is that from the average reservoir pressure to the well flowing pressure. At least two output measurements are required to determine the constants α and β .

The third key element in the discharge analysis method is knowing the pressure at the depth of the pivot point. The pivot point pressure represents the static reservoir pressure at the main feedzone of the well, denoted by \bar{p} . To obtain the pivot point pressure, at least two pressure surveys must be made in the well during warm-up. The pivot point depth is the only point in the well where the pressure remains constant during warm-up (Grant and others, 1983). In wells with one major feedzone the pivot point and the feedzone are at the same depth. In wells with two major feedzones the pivot point will be located between the feedzones according to the lever rule; the point being closer to the higher productivity index feedzone.

The following data are required in the discharge analysis method:

- (a) One output (discharge) measurement giving total mixture enthalpy. The fluid chemistry should also be included to obtain the liquid density and the amount of non-condensable gases.

* feedzone pressure) and wellbottom flowing pressure, respectively.

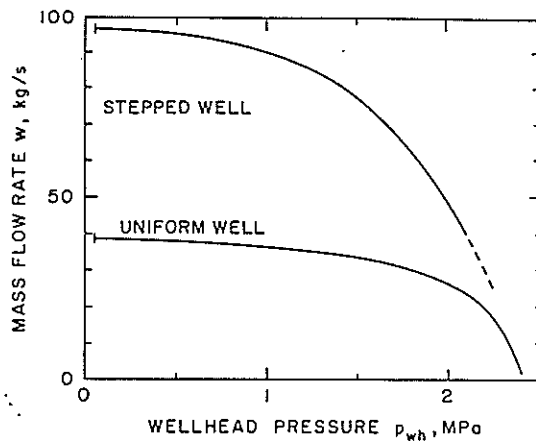


Figure 7. Output curves for uniform and stepped wells in a Brawley-type reservoir.

- (b) Two pressure profiles in the static well during warm-up to determine the pivot point that represents the average reservoir pressure at that depth.
- (c) Well and casing design for depth, diameter, and roughness.

The following calculations are carried out in the discharge analysis method using a wellbore simulator:

- (a) Starting from the wellhead, calculate the flowing pressure profile down to the depth of the pivot point. This gives p_{wf} , the flowing wellbore pressure.
- (b) Calculate productivity index using the measured flowrate w and the pressure values \bar{p} and p_{wf} already obtained.
- (c) Using the productivity index determined, calculate the flowing wellbore pressure for some new flowrate; higher or lower.
- (d) Starting from the depth of the pivot point and using the new wellbore flowing pressure, calculate the pressure (and temperature) profile to the wellhead. This gives a new wellhead pressure.

Repeating steps (c) and (d) of the calculations, it becomes possible to determine the wellhead pressure at different flowrates, and to construct an output curve.

Output data from well 12 in the Svartsengi field in Iceland can be used to illustrate the discharge analysis method. Pressure surveys were taken in well 12 before it was discharged for the first time, after 10 days and 3 months of warm-up. The pressure profiles in Figure 8 are shown to intersect in the depth range 1000-1200 m (Gudmundsson, 1984). This intersection is called the pivot point and represents the pressure controlling depth of the well. Well 12 was discharged for a few weeks and the massflow stabilized at 42 kg/s and a wellhead pressure of 1500 kPa. The steam-brine enthalpy was measured 1000 kJ/kg, which corresponds to a liquid water temperature of 232°C.

The pivot point pressure (average reservoir pressure \bar{p}) was taken as 1279 psia at 3936 ft. depth. The casing inside diameter was 1.0521 ft. to 607 m and the open hole (bare-foot) diameter 1.0208 ft. to the bottom at 1477 m. The total flowrate was taken as 330,000 lb/hr at 220 psia wellhead pressure and the mixture enthalpy as 429 Btu/lb.

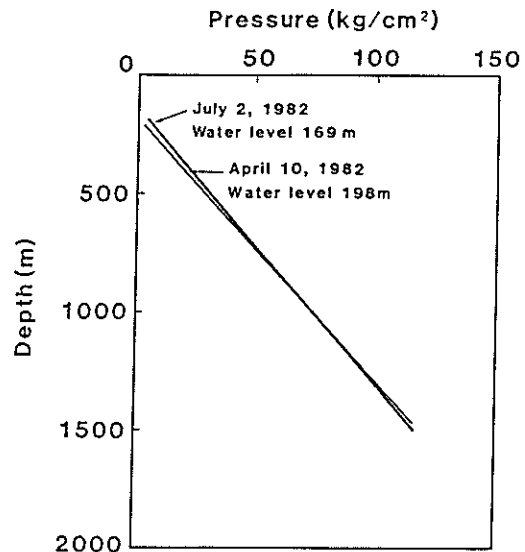


Figure 8. Pressure profiles during warm-up in well 12 in the Svartsengi field, Iceland.

Using a state-of-the-art wellbore simulator (Ortiz-R., 1983), the flowing pressure at the pivot point was calculated $p_{wf} = 1050$ psia. For the given flowrate w (lb/hr) and average reservoir pressure \bar{p} , the productivity index was determined $P.I. = 1456$ lb/hr.psi. The wellhead pressure was then calculated for a range of flowrates. The results of the wellbore simulation calculations for well 12; are shown in Figure 9. In addition to the estimated output (discharge) curve, the pressures assumed and calculated downhole are also shown. These are the reservoir, feedzone, and flashing pressures. Note that the flashing pressure is the saturation pressure corresponding to the enthalpy of the geothermal fluid. What the figure shows is that the potential pressure drop dominates the discharge behavior of the well. Friction losses contribute some pressure drop in the two-phase region, but only above 600,000-800,000 lb/hr flowrate.

Deliverability

The production of steam and water from a geothermal reservoir is a series problem. That is, it depends on the reservoir pressure, the flow of fluid through the feedzone into the well, and then up the wellbore to the surface. These three elements of deliverability are called reservoir, inflow, and wellbore performance, respectively. An output test of a geothermal well gives the deliverability at the time of testing. After a few years of production the deliverability is likely to change because of drawdown in reservoir

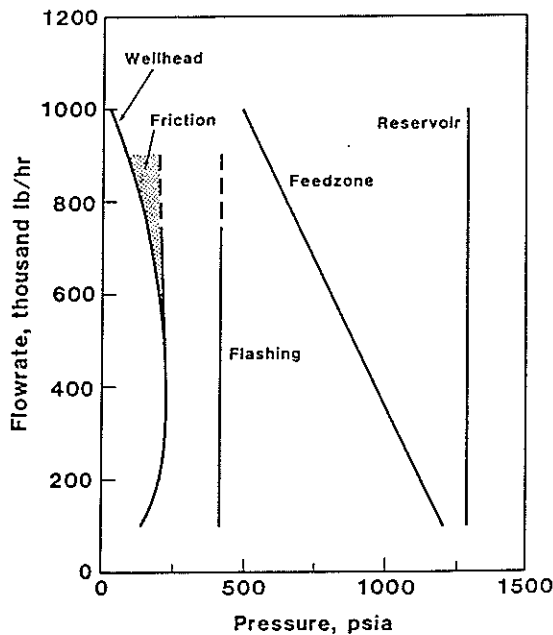


Figure 9. Output curve and downhole pressures in well 12 in Svartsengi field, Iceland.

pressure. The prediction of reservoir pressure with time is the subject of reservoir modeling, and will not be discussed here.

The flow behavior of a typical geothermal reservoir-wellbore system is shown in Figure 10 (Marcou, 1985). The family of curves that go from high to low wellbore flowing pressure p_{wf} are the inflow performance. The highest curve, for example, is the inflow performance before any reservoir pressure drawdown has occurred. The figure shows an initial reservoir pressure of 9 MPa at zero flowrate. With time the reservoir pressure falls and so does the mass flowrate. The inflow performance curves in Figure 10 are composed of two forms of flow behavior, depending upon whether the flowing pressure is above or below the saturation pressure of the geothermal fluid. The saturation pressure is the pressure at which liquid water at a given temperature will start to boil. For the liquid-dominated reservoir conditions used in Figure 10, the saturation pressure is between 4 and 5 MPa (corresponding to reservoir temperature in the range 250 to 260°C). Above the saturation pressure a linear relationship was assumed between the mass flowrate w and well flow pressure p_{wf} ; that is, a laminar flow productivity index as used in the discharge analysis example above. Below the saturation pressure, however, the slope of the inflow performance curve was assumed to become more and more negative. This indicates that when a steam-water mixture enters the wellbore, the resistance to flow is greater than for liquid-only flow at the same mass flowrate. In the petroleum industry, a solution-gas drive reservoir is not unlike a geothermal

steam-water flashing reservoir. The empirical inflow performance relationship of Vogel (1968) was used to construct the below saturation pressure part of the family of curves in Figure 10. This kind of geothermal inflow performance curve has been matched with success to downhole data from well 14-2 in the Roosevelt Hot Springs field in Utah (Marcou, 1985). The method does not take into consideration the gain in mixture enthalpy that occurs when flashing takes place in the reservoir, as discussed by Menzies and others (1982).

The two curves in Figure 10 that cut across the family of inflow performance curves, are the wellbore performance curves of 9-5/8 in. and 13-3/8 in. production casing, for a given set of wellhead conditions. These curves are also called casing performance curves. They were constructed assuming 1100 kJ/kg enthalpy liquid water flowing from a depth of 900 m to a constant wellhead pressure of 690 kPa (100 psia). This mixture enthalpy corresponds to that of liquid water in the temperature range 250 to 255°C. A wellbore simulator was used to calculate the well flowing pressure at 900 m depth at different mass flowrates for a constant wellhead pressure, such as would be in a situation where steam is separated at or above some constant pipeline (steam

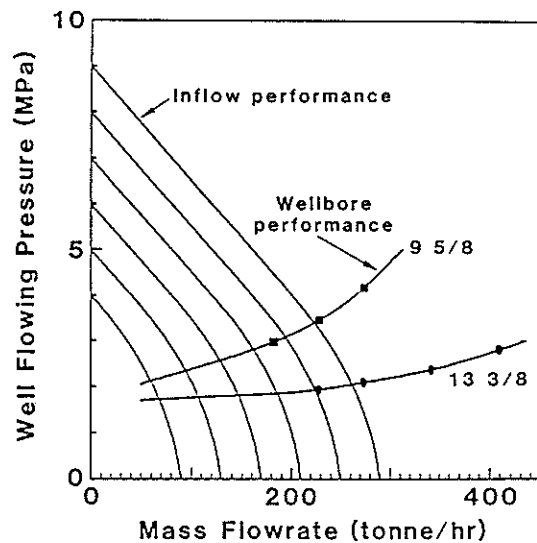


Figure 10. Deliverability behavior of a typical liquid-dominated reservoir-wellbore system.

turbine inlet) pressure. The mass flowrate of steam and water from the geothermal reservoir-wellbore system shown in Figure 10, is determined by the intersection of the inflow and wellbore performance curves. For example, the highest pressure inflow curve intersect the 9-5/8 in. and 13-3/8 in. wellbore curves at 220 and 260 tonne/hr flowrates, respectively. In this way the mixture flowrate at the wellhead can be determined with time as the inflow performance curves become lower.

The slopes of the inflow and wellbore performance curves in Figure 10 are such that increasing the casing diameter from 9- $\frac{5}{8}$ in. to 13- $\frac{5}{8}$ in. increases the mass flowrate by only 18 percent (from 61 to 72 kg/s). This increase is much less than that demonstrated in the Svartsengi field in Iceland and shown in Figure 5. The reason for this is that the inflow performance used in Figure 10 is that of a typical geothermal well, using well 14-2 in the Roosevelt Hot Springs field as an example. The wells in the Svartsengi field, however, attain much greater production rates because of higher reservoir and feedzone permeability. The linear productivity index corresponding to the inflow performance in Figure 10 is about 40 percent of that reported for well 12 in the Svartsengi field above. A higher productivity index means that the well flowing pressure shown in Figure 10 falls less rapidly with increasing mass flowrate. Therefore, it will intersect the wellbore performance curves at a higher flowrate.

Summary

- (a) Typical two-phase geothermal wells produce sufficient steam to generate about 5 MW of electric power.
- (b) Two-phase mixtures with excess enthalpy can flow into the wellbore. The steam fraction of such wells at the wellhead can range from that of liquid feed-zone wells, to dry or even superheated steam wells.
- (c) Larger diameter casing allows greater production rates in typical geothermal fields. Under favorable reservoir conditions the rate of production is proportional to the casing cross sectional area.
- (d) Discharge analysis is a method to estimate the output curve of two-phase liquid feed wells from the minimum of data.
- (e) The deliverability of steam and water from a geothermal system depends on coupling of the reservoir, inflow, and wellbore performances.

References

- Bilicki, Z., DiPippo, R., Kestin J., Maeder, P.F. & Micaelides, E.E.: *Available work analysis in the design of geothermal wells*, Proc., Int'l. Conf. Geoth. Energy, Florence, Italy, May 11-14, 1985, vol. 2, 227-248.
- Budd, C.F.: *Steam production at The Geysers geothermal field*, Geothermal energy, P. Kruger & C. Otte (eds.), Stanford University Press, Stanford, California (1973).
- Gould, T.L.: *Vertical two-phase steam-water flow in geothermal wells*, J. Pet. Tech. (Aug. 1974), 833-842.
- Grant, M.A., Bixley, P.F. & Donaldson, I.G.: *Internal flows in geothermal wells: Their identification and effect on the wellbore temperature and pressure profiles*, S.P.E.J., Feb. 1983, 168-176.
- Grant, M.A., Donaldson, I.G. & Bixley, P.R.: *Geothermal reservoir engineering*, Academic Press, New York, (1982).
- Grant, M.A. & Glover, R.B.: *Two-phase heat and mass transfer experiment at well BR21 Broadlands*, Geothermics 13 (1984), 193-213.
- Gudmundsson, J.S., Ortiz-R., J. & Granados, E.: *Two-phase flow and calcite deposition in geothermal wells*, Paper SPE-12741, SPE of AIME California Regional Meeting, Long Beach, California, April, 1984.
- Gudmundsson, J.S., *Discharge Analysis Method for Two-Phase Geothermal Wells*, Geoth. Resources Council Transactions, vol. 8, 295-299, Reno, NV, August 26-29, 1984.
- Gudmundsson, J.S., Thorhallsson, S. & Ragnars, K.: *Status of geothermal electric power in Iceland 1980*, Proc., 5th Geoth. Conf. Workshop, Electric Power Research Institute, Report AP-2098, Nov. 1981, 7.52-7.65.
- James, R.: *Factors controlling borehole performance*, Geothermics, Special Issue 2 (1970), 1502-1515.
- James, R.: *Locus of wellhead pressure with time under production discharge*, Proc., 5th New Zealand Geothermal Workshop, Auckland, New Zealand (1983), 109-111.
- Marcou, J.A.: *Optimizing development strategy for liquid dominated geothermal reservoirs*, Stanford Geothermal Program, Report SGP-TR-90, Stanford, California (1985).
- Menzies, A.J., Gudmundsson, J.S. & Horne, R.N.: *Flashing flow in fractured geothermal reservoirs*, Proc., Eighth, Workshop Geoth. Reservoir Engineering, SGP-TR-60, Stanford, California (1982), 143-147.
- Miller, C.W. & Harrison, R.: *Using Wellbore Models in the Development of Geothermal Resources*, Geoth. Resources Council Bulletin (May 1985), 17-21.
- Molinar-C., R.: Private communication (1985).
- Nathenson, M.: *Flashing flow in hot-water geothermal wells*, J. Research U.S. Geol. Survey, v. 2, Nov.-Dec. 1974, 743-751.
- Nind, T.E.W.: *Principles of oil well production*, McGraw-Hill Book Company, New York (1981), LP.
- Ortiz-R., J.: *Two-phase flow in geothermal wells: Development and uses of a computer code*, Stanford Geothermal Program, Report SGP-TR-66, June 1983.
- Stefansson, V. & Steingrimsson, B.: *Production characteristic of wells tapping two-phase reservoirs at Krafla and Namafjall*, Proc., Sixth Workshop Geoth. Reservoir Engineering, SGP-TR-50, Stanford, California (1980), 49-59.
- Upadhyay, R.N., Hartz, J.D., Tomkoria, B.N. & Gulati, M.S.: *Comparison of calculated and observed pressure drops in geothermal wells producing steam-water mixtures*, Paper SPE-6766, 52nd Annual Fall Tech. Conf. Exhibition, Denver, Colorado, Oct. 1977.
- Vogel, J.V.: *Inflow performance relationships for solution-gas drive reservoirs*, J. Pet. Tech. (Jan. 1968), 83. □